

Spin-orbit precession along eccentric orbits: improving the knowledge of self-force corrections and of their effective-one-body counterparts

Donato Bini¹, Thibault Damour², Andrea Geralico¹

¹*Istituto per le Applicazioni del Calcolo “M. Picone,” CNR, I-00185 Rome, Italy*

²*Institut des Hautes Études Scientifiques, 91440 Bures-sur-Yvette, France.*

The (first-order) gravitational self-force correction to the spin-orbit precession of a spinning compact body along a slightly eccentric orbit around a Schwarzschild black hole is computed through the ninth post-Newtonian order, improving recent results by Kavanagh et al. [Phys. Rev. D **96**, 064012 (2017).] This information is then converted into its corresponding Effective-One-Body counterpart, thereby determining several new post-Newtonian terms in the gyrogravitomagnetic ratio g_{S*} .

I. INTRODUCTION

In the newly born gravitational wave (GW) era [1–4], it will become more and more important to extract accurate physical information from experimental data as rapidly as possible. This implies constantly improving the mathematical modelling of the dynamics, and of the gravitational-wave emission, of inspiralling and coalescing binary systems. One of the current key methods used in the LIGO-Virgo data analysis pipelines, is the Effective-One-Body (EOB) formalism [5–9]. The EOB formalism is used both in the construction of hundreds of thousands of semi-analytical templates [10–12], describing the complete waveform emitted by coalescing binary black holes, and in the construction of hybrid EOB-numerical waveforms that are then used to calibrate frequency-domain phenomenological waveforms [13].

The EOB approach is based, among other building blocks, on the definition of an analytical, resummed Hamiltonian which allows one to describe the coalescence process up to the merger of the two considered bodies. It is useful both for binary black hole systems, and for systems comprising neutron stars [14–16]. In recent years the necessity of making EOB theory more efficient has been driving research in several analytical directions which can potentially improve the accuracy of the EOB dynamics. In particular, new knowledge acquired through Post-Newtonian (PN) theory (valid in the weak-field and slow motion regime), gravitational self-force (SF) theory (valid when the mass ratio of the two bodies is very small), Post-Minkowskian (PM) theory (valid in the weak field regime), and numerical relativity (NR), has been usefully transcribed in terms of the basic potentials entering the EOB Hamiltonian. For instance, the current, fourth post-Newtonian (4PN) knowledge [17–20] has been translated in EOB terms in Ref. [21]. For examples of the translation of high-PN-order SF knowledge into EOB counterparts, see, e.g., Refs. [22–25].

The aim of the present paper is to improve the current analytical knowledge of *eccentricity-dependent* contributions to the spin-orbit precession of a spinning compact body orbiting a nonspinning black hole, and to translate this knowledge within the EOB formalism. The computation of gauge-invariant, eccentricity-dependent SF effects in the spin-orbit precession of a small spinning

body was initiated in a recent paper by Akcay, Dempsey and Dolan [26]. Then Kavanagh et al. [25] analytically computed the PN expansion of the self-force correction to the spin-orbit precession, up to the sixth PN order and transcribed this information into the corresponding knowledge of the PN expansion of the (phase-space-dependent) EOB gyrogravitomagnetic ratio $g_{S*}(r, p_r, p_\phi)$ up to the fourth PN order in the coefficient of the square of the radial momentum, i.e. $O(u^4 p_r^2)$ included (where $u = GM/(c^2 r)$).

Here we shall extend the work done in Ref. [25] to the ninth PN level for the spin precession, at the second order in eccentricity, almost doubling the number of the analytically known terms (because of the presence of many half-PN-order contributions). We shall then explicitly derive the relationship between the spin precession invariant along eccentric orbits, and the various potentials parametrizing spin-orbit effects within the EOB formalism, thereby determining the PN expansion of the $O(p_r^2)$ contribution to the gyrogravitomagnetic ratio $g_{S*}(r, p_r, p_\phi)$ up to the fractional seventh PN accuracy (i.e. an improvement by six half-PN-order contributions).

To make the paper self consistent we will start by briefly recalling the main computational steps of Refs. [26] and [25]. Most of the technical details will, however, be relegated to an appendix. Unless differently specified we will use units so that $c = G = 1$.

II. FIRST-ORDER SF SPIN-PRECESSION INVARIANT $\Delta\psi(u_p, e)$

In this section we recall the basic theory underlying the derivation of the spin precession invariant $\psi(m_2\Omega_r, m_2\Omega_\phi; m_1/m_2)$, and its first-order SF contribution $\Delta\psi$. Consider a binary system consisting of a spinning compact body (of mass m_1 and spin S_1) and a Schwarzschild black hole (of mass m_2 and spinless, $S_2 = 0$) with $q \equiv \frac{m_1}{m_2} \ll 1$. Through $O(m_1)$, the small body can be considered as following an eccentric geodesic orbit in a (regularized) perturbed spacetime $g_{\alpha\beta}^R$, while its associated spin vector is parallelly-transported in $g_{\alpha\beta}^R$. Here we consider the small-spin regime $|S_1|/(cGm_1^2) \ll 1$, i.e. we work linearly in S_1 . The regularized perturbed

metric $g_{\alpha\beta}^R$ is decomposed as

$$g_{\alpha\beta}^R = \bar{g}_{\alpha\beta} + q h_{\alpha\beta}^R + O(q^2), \quad (2.1)$$

where $\bar{g}_{\alpha\beta}$ is the background spacetime

$$\begin{aligned} d\bar{s}^2 &= \bar{g}_{\alpha\beta} dx^\alpha dx^\beta \\ &= -f dt^2 + \frac{1}{f} dr^2 + r^2(d\theta^2 + \sin^2\theta d\phi^2), \end{aligned} \quad (2.2)$$

with $f = 1 - \frac{2m_2}{r}$, and where $q h_{\alpha\beta}^R$ is the first-order SF metric perturbation. Henceforth, we shall omit the superscript R. Let us denote by $\Omega_r = 2\pi/T_r$ and $\Omega_\phi = \Phi/T_r$ the radial and (averaged) azimuthal angular frequencies, respectively. Here, Φ denotes the accumulated azimuthal angle from periapsis to periapsis. The spin precession is conveniently measured by the dimensionless quantity

$$\psi(m_2\Omega_r, m_2\Omega_\phi; q) = 1 - \frac{\Psi}{\Phi}, \quad (2.3)$$

defined by the ratio of the amount of precession angle Ψ (with respect to a polar-type basis) accumulated by the spin vector over one radial period T_r , to the accumulated periastron precession angle Φ .

Akcay, Dempsey and Dolan [26] showed how to calculate the $O(q)$, SF contribution to the gauge-invariant function $\psi(m_2\Omega_r, m_2\Omega_\phi; q)$, i.e. (taking into account that Φ is the same for the perturbed, $q \neq 0$, and background, $q = 0$, orbits),

$$\begin{aligned} \Delta\psi &= \frac{1}{q} [\psi(m_2\Omega_r, m_2\Omega_\phi; q) - \psi(m_2\Omega_r, m_2\Omega_\phi; 0)] \\ &= -\frac{\Delta\Psi}{\Phi}, \end{aligned} \quad (2.4)$$

with

$$\Delta\Psi = \frac{1}{q} [\Psi(m_2\Omega_r, m_2\Omega_\phi; q) - \Psi(m_2\Omega_r, m_2\Omega_\phi; 0)]. \quad (2.5)$$

See Ref. [26], and the Appendix below, for the procedure needed to compute $\Delta\Psi$ for fixed values of the two frequencies (Ω_r, Ω_ϕ) . After the computation of the function $\Delta\psi(\Omega_r, \Omega_\phi)$, one can reexpress it as a function of the inverse semi latus rectum $u_p = 1/p$, and eccentricity e , of the unperturbed orbit.

Kavanagh et al. [25] have recently calculated, following the approach of Ref. [26], the spin-precession invariant $\Delta\psi(u_p, e)$ up to order $O(e^2)$ in a small-eccentricity expansion, $e \ll 1$, and up to order $O(u_p^6)$ in the PN expansion, $u_p = 1/p \ll 1$. Their calculation was based on a computation (via the Teukolsky formalism) of the PN-expanded metric perturbation in the radiation gauge. We closely follow their analysis, extending the calculation of $\Delta\psi$ up to the order $O(u_p^9)$ included. Our final result for the spin precession invariant $\Delta\psi(u_p, e)$ reads

$$\begin{aligned} \Delta\psi(u_p, e) &= \Delta\psi^{(0)}(u_p) + e^2 \Delta\psi^{(2)}(u_p) \\ &\quad + e^4 \Delta\psi^{(4)}(u_p) + \mathcal{O}(e^6), \end{aligned} \quad (2.6)$$

where the PN structure of $\Delta\psi^{(2)}(u_p)$ is (note the half-PN-order terms $c_{k+\frac{1}{2}}, c_{k+\frac{1}{2}}^{\ln}, \dots$)

$$\begin{aligned} \Delta\psi^{(2)}(u_p) &= \sum_{k \geq 2} c_k^c u_p^k + \ln u_p \sum_{k \geq 4} c_k^{\ln} u_p^k \\ &\quad + \sum_{k \geq 5} c_{k+\frac{1}{2}} u_p^{k+\frac{1}{2}} + \ln^2 u_p \sum_{k \geq 7} c_k^{\ln^2} u_p^k \\ &\quad + \ln u_p \sum_{k \geq 8} c_{k+\frac{1}{2}}^{\ln} u_p^{k+\frac{1}{2}} + \dots, \end{aligned} \quad (2.7)$$

and explicitly

$$\begin{aligned} \Delta\psi^{(2)}(u_p) &= u_p^2 - \left(\frac{123}{256} \pi^2 - \frac{341}{16} \right) u_p^3 \\ &\quad - \left(\frac{164123}{480} - \frac{536}{5} \gamma - \frac{268}{5} \ln(u_p) + \frac{23729}{4096} \pi^2 + \frac{10206}{5} \ln(3) - \frac{11720}{3} \ln(2) \right) u_p^4 \\ &\quad - \left(\frac{4836254}{105} \ln(2) - \frac{21333485}{49152} \pi^2 - \frac{9765625}{1344} \ln(5) + \frac{22682}{15} \gamma + \frac{89576921}{57600} + \frac{11341}{15} \ln(u_p) \right. \\ &\quad \left. - \frac{4430133}{320} \ln(3) \right) u_p^5 + \frac{319609}{630} \pi u_p^{11/2} \\ &\quad - \left(\frac{17193359375}{145152} \ln(5) - \frac{32088966503}{2359296} \pi^2 + \frac{2508913}{1890} \ln(u_p) - \frac{273329813}{945} \ln(2) \right. \\ &\quad \left. + \frac{159335343}{8960} \ln(3) + \frac{146026515}{1048576} \pi^4 + \frac{464068669129}{5080320} + \frac{2508913}{945} \gamma \right) u_p^6 \end{aligned}$$

$$\begin{aligned}
& - \frac{1586616631}{235200} \pi u_p^{13/2} \\
& - \left(\frac{39826256}{315} \ln(u_p) \ln(2) + \frac{2888955324477314921}{2347107840000} - \frac{1075057978433}{9702000} \ln(u_p) - \frac{678223072849}{6082560} \ln(7) \right. \\
& \quad + \frac{79652512}{315} \gamma \ln(2) - \frac{15912612}{175} \ln(2) \ln(3) + \frac{7219504}{525} \gamma \ln(u_p) - \frac{2411543359375}{2838528} \ln(5) \\
& \quad - \frac{7956306}{175} \ln(3)^2 - \frac{2387982140729}{8731800} \ln(2) - \frac{1075057978433}{4851000} \gamma - \frac{465082867177871}{6606028800} \pi^2 \\
& \quad + \frac{1804876}{525} \ln(u_p)^2 - \frac{15912612}{175} \gamma \ln(3) + \frac{299782486660473}{275968000} \ln(3) + \frac{7219504}{525} \gamma^2 \\
& \quad - \frac{314165501411}{335544320} \pi^4 + \frac{80263696}{175} \ln(2)^2 - \frac{134944}{5} \zeta(3) - \frac{7956306}{175} \ln(u_p) \ln(3) \Big) u_p^7 \\
& + \frac{2404331748779}{279417600} \pi u_p^{15/2} \\
& - \left(\frac{3173828125}{7056} \ln(2) \ln(5) - \frac{19171249336}{11025} \ln(u_p) \ln(2) + \frac{3173828125}{7056} \gamma \ln(5) + \frac{621149553}{784} \gamma \ln(3) \right. \\
& \quad - \frac{12590844685671737819611}{939781979136000} + \frac{33310259864964463}{443925135360} \pi^2 + \frac{3972491619599291}{5297292000} \ln(u_p) \\
& \quad - \frac{812331139710343959}{100452352000} \ln(3) + \frac{3173828125}{14112} \ln(u_p) \ln(5) - \frac{38342498672}{11025} \gamma \ln(2) + \frac{5551264}{21} \zeta(3) \\
& \quad + \frac{55100101995388051}{23721984000} \ln(7) + \frac{621149553}{784} \ln(2) \ln(3) + \frac{3173828125}{14112} \ln(5)^2 + \frac{88630614687481099}{7945938000} \ln(2) \\
& \quad + \frac{3978068608616891}{2648646000} \gamma - \frac{371280152}{2205} \gamma \ln(u_p) + \frac{621149553}{1568} \ln(u_p) \ln(3) + \frac{621149553}{1568} \ln(3)^2 - \frac{371280152}{2205} \gamma^2 \\
& \quad + \frac{196313675703125}{21697708032} \ln(5) + \frac{31118085613898053}{257698037760} \pi^4 - \frac{7893208952}{1225} \ln(2)^2 - \frac{92820038}{2205} \ln(u_p)^2 \Big) u_p^8 \\
& - \left(- \frac{21157957560083191439}{33563642112000} \pi + \frac{166628746}{315} \pi \ln(2) + \frac{6610847233}{165375} \pi \ln(u_p) + \frac{13221694466}{165375} \pi \gamma \right. \\
& \quad - \frac{926441631}{6125} \pi \ln(3) - \frac{123567238}{4725} \pi^3 \Big) u_p^{17/2} \\
& - \left(\frac{89957972}{315} \zeta(3) - \frac{113231016807891871}{5175705600} \ln(7) + \frac{47576994975313901}{21189168000} \gamma + \frac{72839234785800578877}{4419903488000} \ln(3) \right. \\
& \quad + \frac{1362682591}{19845} \ln(u_p)^2 + \frac{1590291075741430578125}{33141699182592} \ln(5) - \frac{27467645056526844769}{419545526400} \ln(2) \\
& \quad - \frac{962681186487}{268435456} \pi^6 + \frac{5450730364}{19845} \gamma \ln(u_p) + \frac{11600054253556}{1091475} \ln(u_p) \ln(2) + \frac{23200108507112}{1091475} \gamma \ln(2) \\
& \quad - \frac{873170066079}{1724800} \ln(u_p) \ln(3) + \frac{815583044961}{862400} \ln(2) \ln(3) - \frac{873170066079}{862400} \gamma \ln(3) - \frac{28312548828125}{3592512} \gamma \ln(5) \\
& \quad - \frac{28312548828125}{3592512} \ln(2) \ln(5) - \frac{28312548828125}{7185024} \ln(u_p) \ln(5) - \frac{873170066079}{1724800} \ln(3)^2 \\
& \quad + \frac{399034285145396}{9823275} \ln(2)^2 + \frac{5450730364}{19845} \gamma^2 + \frac{47354559565317101}{42378336000} \ln(u_p) \\
& \quad - \frac{1632714242298331008005890223}{2638907797413888000} - \frac{28312548828125}{7185024} \ln(5)^2 - \frac{517077970581977291}{2959500902400} \pi^2 \\
& \quad + \frac{411339398981140702321}{65970697666560} \pi^4 \Big) u_p^9 + O_{\ln}(u_p^{19/2}). \tag{2.8}
\end{aligned}$$

When comparing with the lower-accuracy result of Ref. [25], one should note that the whole $O(u_p^5)$ term was misprinted there (as being simply exactly the same as the $O(u_p^4)$ term). The terms from $u_p^{13/2}$ (included) up to u_p^9 (included) are new with this work, and represent one of

the main outcomes of the present paper.

The zero-eccentricity term $\Delta\psi^{(0)}(u_p)$ in Eq. (2.6) is related, as shown in [26], to the spin precession invariant $\Delta\psi_{(\text{circ})}(u_p)$ directly computed along circular orbits [23,

27–29] via

$$\begin{aligned}\Delta\psi^{(0)}(u_p) &= \Delta\psi_{\text{(circ)}}(u_p) \\ &+ \frac{1}{4} \frac{(1-3u_p)^{1/2}(1-6u_p)}{1-\frac{39}{4}u_p+\frac{43}{2}u_p^2} (\rho(u_p) - 4u_p),\end{aligned}\quad (2.9)$$

where $\rho(u_p)$ is the EOB function measuring the periastron precession at the 1SF-level [30, 31]. [Note that the expression for $\Delta\psi_{\text{(circ)}}(y)$ given in Ref. [28] is incorrect for the fractional power terms $y^{19/2}$ and beyond.]

The higher-order-in-eccentricity contributions to $\Delta\psi(u_p, e)$, starting from $e^4\Delta\psi^{(4)}(u_p)$, present an analytical challenge that we leave to future work. The present knowledge of $\Delta\psi(u_p, e)$ beyond the $O(e^2)$ level consists of the lowest-PN-order $O(e^4)$ term (derived in Ref. [26]), namely

$$\Delta\psi^{(4)}(u_p) = -\frac{1}{2}u_p^3. \quad (2.10)$$

III. IMPROVING THE KNOWLEDGE OF THE EOB GYROGRAVITOMAGNETIC RATIO

$$g_{S*}(u, p_r, p_\phi)$$

In EOB theory, the total Hamiltonian of a two-body system is expressed in terms of the “effective EOB Hamiltonian”, H_{eff} , via

$$\begin{aligned}H(\mathbf{R}, \mathbf{P}, \mathbf{S}_1, \mathbf{S}_2) &= Mc^2 \sqrt{1 + 2\nu \left(\frac{H_{\text{eff}}}{\mu c^2} - 1 \right)} \\ &\equiv Mc^2 h,\end{aligned}\quad (3.1)$$

where

$$\begin{aligned}M &= m_1 + m_2, \quad \mu = \frac{m_1 m_2}{m_1 + m_2}, \\ \nu &= \frac{\mu}{M} = \frac{m_1 m_2}{(m_1 + m_2)^2}.\end{aligned}\quad (3.2)$$

When considering spinning bodies, the effective EOB Hamiltonian H_{eff} is decomposed into the sum of an orbital part and a spin-orbit part

$$H_{\text{eff}} = H_{\text{eff}}^{\text{O}} + H_{\text{eff}}^{\text{SO}}. \quad (3.3)$$

Here, we work linearly in the spins, so that the orbital part $H_{\text{eff}}^{\text{O}}$ will be independent of the spins, while the spin-orbit part will be linear in the spins. The structure of the *orbital* part is

$$H_{\text{eff}}^{\text{O}} = c^2 \sqrt{A \left(\mu^2 c^2 + \mathbf{P}^2 + \left(\frac{1}{B} - 1 \right) P_R^2 + Q \right)}, \quad (3.4)$$

where

$$\mathbf{P}^2 = \frac{P_R^2}{B} + \frac{\mathbf{L}^2}{R^2} = \frac{P_R^2}{B} + \frac{P_\phi^2}{R^2}. \quad (3.5)$$

Here $\mathbf{L} = \mathbf{R} \times \mathbf{P}$ denotes the orbital angular momentum ($|\mathbf{L}| \equiv P_\phi$), $A(R)$ and $B(R)$ are the two main EOB radial potentials and the phase-space extra potential $Q(R, P_R)$ is at least quartic in the radial momentum P_R . The structure of the spin-orbit part of the effective Hamiltonian is

$$\begin{aligned}H_{\text{eff}}^{\text{SO}} &= G_S^{\text{phys}}(R, P_R^2, \mathbf{L}^2) \mathbf{L} \cdot \mathbf{S} \\ &+ G_{S*}^{\text{phys}}(R, P_R^2, \mathbf{L}^2) \mathbf{L} \cdot \mathbf{S}_*.\end{aligned}\quad (3.6)$$

It involves the following two symmetric combination of the spin vectors \mathbf{S}_1 and \mathbf{S}_2 of the system

$$\mathbf{S} \equiv \mathbf{S}_1 + \mathbf{S}_2, \quad \mathbf{S}_* \equiv \frac{m_2}{m_1} \mathbf{S}_1 + \frac{m_1}{m_2} \mathbf{S}_2. \quad (3.7)$$

In the parallel-spin case $\mathbf{L} \cdot \mathbf{S} = LS = P_\phi S$ and $\mathbf{L} \cdot \mathbf{S}_* = LS_* = P_\phi S_*$. It is convenient to work with the following dimensionless variables

$$\begin{aligned}r &= \frac{c^2 R}{GM}, \quad u = \frac{GM}{c^2 R} \equiv \frac{1}{r}, \quad j \equiv p_\phi = \frac{cP_\phi}{GM\mu}, \\ p_r &= \frac{P_R}{\mu c}, \quad \hat{Q} = \frac{Q}{\mu^2 c^2},\end{aligned}\quad (3.8)$$

as well as

$$\hat{H}_{\text{eff}} = \frac{H_{\text{eff}}}{\mu c^2} \equiv \hat{H}_{\text{eff}}^{\text{O}} + \hat{H}_{\text{eff}}^{\text{SO}}. \quad (3.9)$$

The Finslerlike contribution \hat{Q} has the structure

$$\hat{Q} = \nu \sum_{n=2}^{\infty} q_{2n}(u) p_r^{2n} + O(\nu^2). \quad (3.10)$$

As we work linearly in the spins, we can replace the dimensionfull spin-orbit coupling functions, G_S^{phys} and G_{S*}^{phys} , entering $H_{\text{eff}}^{\text{SO}}$ by the corresponding dimensionless gyrogravitomagnetic ratios g_S and g_{S*} defined as

$$\begin{aligned}g_S(u, p_r, p_\phi) &= R^3 G_S^{\text{phys}}, \\ g_{S*}(u, p_r, p_\phi) &= R^3 G_{S*}^{\text{phys}}.\end{aligned}\quad (3.11)$$

Here, we shall parametrize the SF expansions (i.e. expansions in powers of ν) of g_S and g_{S*} as

$$\begin{aligned}g_S(u, p_r, p_\phi; \nu) &= 2 + O(\nu), \\ g_{S*}(u, p_r, p_\phi; \nu) &= g_{S*}^{(\nu^0)}(u, p_r, p_\phi) + \nu g_{S*}^{(\nu^1)}(u, p_r) \\ &\quad + \nu^2 g_{S*}^{(\nu^2)}(u, p_r) + \dots\end{aligned}\quad (3.12)$$

with the test-mass limit of $g_{S*}(u, p_r, p_\phi)$ written in the form [32, 33]

$$g_{S*}^{(\nu^0)}(u, p_r, p_\phi) = \frac{2}{1 + \frac{1}{\sqrt{1-2u}}} \frac{1}{\tilde{R}} + \frac{1}{1 + \tilde{R}}, \quad (3.13)$$

where

$$\tilde{R}(u, p_r, p_\phi) = [1 + p_\phi^2 u^2 + (1 - 2u)p_r^2]^{1/2}. \quad (3.14)$$

In the SF expansion of $g_{S*}(u, p_r, p_\phi; \nu)$ (second equation in Eq. (3.12)), we have made a specific gauge-choice for the phase-space dependence of the SF contributions: namely, following the spirit of Ref. [34], we have represented them as functions of u and p_r , without allowing for a dependence on p_ϕ . The first-order self-force (1SF) contribution to g_{S*} can then be expanded in (even) powers of the radial momentum:

$$g_{S*}^{(\nu^1)}(u, p_r) = g_{S*}^{1\text{SF}0}(u) + g_{S*}^{1\text{SF}2}(u)p_r^2 + g_{S*}^{1\text{SF}4}(u)p_r^4 + g_{S*}^{1\text{SF}6}(u)p_r^6 + \dots \quad (3.15)$$

In turn, the various coefficients $g_{S*}^{1\text{SF}0}(u)$, $g_{S*}^{1\text{SF}2}(u)$, etc. of this p_r^2 expansion, have PN expansions in u which start as

$$\begin{aligned} g_{S*}^{1\text{SF}0}(u) &= -\frac{3}{4}u - \frac{39}{4}u^2 + \left(-\frac{7987}{192} + \frac{41}{32}\pi^2\right)u^3 \\ &\quad + O(u^4), \\ g_{S*}^{1\text{SF}2}(u) &= -\frac{9}{4} - \frac{9}{4}u - \frac{717}{32}u^2 + O(u^3), \\ g_{S*}^{1\text{SF}4}(u) &= \frac{5}{2} + O(u). \end{aligned} \quad (3.16)$$

Let us introduce the following notation for the coefficients of the various powers of u in the PN expansion of $g_{S*}^{1\text{SF}n}(u)$

$$\begin{aligned} g_{S*}^{1\text{SF}n}(u) &= \sum_{k \geq 1} g_{*nk}^c u^k + \ln u \sum_{k \geq 3} g_{*nk}^{\ln} u^k \\ &\quad + \sum_{k \geq 4} g_{*n(k+\frac{1}{2})} u^{k+\frac{1}{2}} + \ln^2 u \sum_{k \geq 6} g_{*nk}^{\ln^2} u^k \\ &\quad + \ln u \sum_{k \geq 7} g_{*n(k+\frac{1}{2})} u^{k+\frac{1}{2}} \dots \end{aligned} \quad (3.17)$$

Only a few of these coefficients were determined in Ref. [25], namely:

$$\begin{aligned} g_{*22} &= -\frac{717}{32} \\ g_{*23}^c &= \frac{1447441}{960} - \frac{4829}{256}\pi^2 - \frac{16038}{5}\ln(3) \\ &\quad + \frac{46976}{15}\ln(2) - \frac{512}{5}\gamma \\ g_{*23}^{\ln} &= -\frac{256}{5} \\ g_{*24}^c &= -\left[\frac{184655453}{38400}\right]_{\text{corrected}} + \frac{19162}{35}\gamma + \frac{2097479}{8192}\pi^2 \\ &\quad + \frac{454167}{20}\ln(3) - \frac{1081966}{35}\ln(2) \\ g_{*24}^{\ln} &= +\frac{9581}{35}. \end{aligned} \quad (3.18)$$

Note that the first (rational) term in g_{*24}^c was misprinted in Ref. [25] as

$$-\left[\frac{185195453}{38400}\right]_{\text{incorrect}}. \quad (3.19)$$

In the present work, we have derived (by using the relation between the PN expansion (3.17) and the PN expansion of $\Delta\psi^{(2)}$) additional terms in the PN expansion of $g_{S*}^{1\text{SF}2}(u)$, namely:

$$\begin{aligned} g_{*24.5} &= -\frac{714653}{3150}\pi, \\ g_{*25}^c &= \frac{1136089}{210}\gamma - \frac{19531250}{567}\ln(5) - \frac{82368981}{560}\ln(3) + \frac{121254173}{378}\ln(2) + \frac{1322959637}{196608}\pi^2 + \frac{21119805}{524288}\pi^4 \\ &\quad - \frac{2157036100969787}{26604864000}, \\ g_{*25}^{\ln} &= \frac{1136089}{420}, \\ g_{*25}^{\ln^2} &= 0, \\ g_{*25.5} &= \frac{214163953}{100800}\pi, \\ g_{*25.5}^{\ln} &= 0, \\ g_{*25.5}^{\ln^2} &= 0, \\ g_{*26}^c &= -9024\zeta(3) - \frac{62597340649}{485100}\gamma + \frac{129552734375}{266112}\ln(5) - \frac{695576369871}{1232000}\ln(3) - \frac{640198452653}{661500}\ln(2) \\ &\quad - \frac{126056977883647}{4459069440}\pi^2 + \frac{549062083551}{167772160}\pi^4 - \frac{149101504}{1575}\gamma\ln(2) + \frac{2808108}{25}\ln(3)\ln(2) + \frac{2808108}{25}\ln(3)\gamma \\ &\quad - \frac{79378592}{525}\ln(2)^2 + \frac{160928}{35}\gamma^2 + \frac{1404054}{25}\ln(3)^2 + \frac{357317643875067280292753}{1035737850115584000}, \end{aligned}$$

$$\begin{aligned}
g_6^{\ln} &= -\frac{74550752}{1575} \ln(2) + \frac{1404054}{25} \ln(3) + \frac{160928}{35} \gamma - \frac{62597340649}{970200}, \\
g_{*26}^{\ln^2} &= \frac{40232}{35}, \\
g_{*26.5} &= \frac{193000744063}{93139200} \pi, \\
g_{*26.5}^{\ln} &= 0, \\
g_{*26.5}^{\ln^2} &= 0, \\
g_{*27}^c &= \frac{7394848}{35} \zeta(3) - \frac{4747561509943}{15444000} \ln(7) + \frac{16112853388177387}{15891876000} \gamma - \frac{29717454296875}{8805888} \ln(5) \\
&+ \frac{2141915038593471}{448448000} \ln(3) + \frac{5373188171264357}{2270268000} \ln(2) + \frac{36023768285157071}{208089907200} \pi^2 - \frac{9570352156443723}{10737418240} \pi^4 \\
&+ \frac{448804392116006600471071523}{5192955612149760000} + \frac{45230944}{63} \gamma \ln(2) - \frac{23385591}{25} \ln(3) \ln(2) - \frac{23385591}{25} \ln(3) \gamma \\
&+ \frac{19919007824}{11025} \ln(2)^2 - \frac{1722628912}{11025} \gamma^2 - \frac{23385591}{50} \ln(3)^2, \\
g_{*27}^{\ln} &= \frac{16069729193463787}{31783752000} - \frac{1722628912}{11025} \gamma - \frac{23385591}{50} \ln(3) + \frac{22615472}{63} \ln(2), \\
g_{*27}^{\ln^2} &= -\frac{430657228}{11025}. \tag{3.20}
\end{aligned}$$

Summarizing, the present, first-order self-force knowledge of $g_{S*} = g_{S*}^{\text{1SF0}}(u) + g_{S*}^{\text{1SF2}}(u)p_r^2 + g_{S*}^{\text{1SF4}}(u)p_r^4 + O(p_r^6)$ is the following:

$$\begin{aligned}
g_{S*}^{\text{1SF0}}(u) &= -\frac{3}{4}u - \frac{39}{4}u^2 + \left(-\frac{7987}{192} + \frac{41}{32}\pi^2 \right) u^3 \\
&+ \left(-\frac{11447}{120} - 48\gamma - \frac{1456}{15} \ln(2) - 24 \ln(u) + \frac{26943}{2048} \pi^2 \right) u^4 \\
&+ \left(-\frac{729}{7} \ln(3) + \frac{4216}{35} \ln(u) + \frac{8432}{35} \gamma + \frac{62296}{105} \ln(2) + \frac{1404359}{8192} \pi^2 - \frac{487501139}{268800} \right) u^5 \\
&- \frac{93304}{1575} \pi u^{11/2} \\
&+ \left(\frac{447572}{2835} \ln(u) + \frac{895144}{2835} \gamma - \frac{1937576}{2835} \ln(2) + \frac{37179}{35} \ln(3) + \frac{16790137}{1048576} \pi^4 - \frac{1780964579}{7077888} \pi^2 \right. \\
&\quad \left. - \frac{15354135144661823}{11732745024000} \right) u^6 \\
&+ \frac{3928339}{12600} \pi u^{13/2} \\
&+ \left(\frac{14552}{105} \ln(u)^2 - \frac{197060521717}{33544320} \pi^4 - \frac{30895906513}{8731800} \ln(u) - \frac{30895906513}{4365900} \gamma + \frac{499904}{225} \ln(2) \gamma \right. \\
&\quad \left. - \frac{6007689}{1760} \ln(3) + \frac{448438768980344811772817}{53858368206010368000} + \frac{1167584}{525} \ln(2)^2 - \frac{17567377338739}{8918138880} \pi^2 + \frac{58208}{105} \gamma \ln(u) \right. \\
&\quad \left. - 1088\zeta(3) - \frac{1953125}{3564} \ln(5) - \frac{22149706021}{3118500} \ln(2) + \frac{58208}{105} \gamma^2 + \frac{249952}{225} \ln(2) \ln(u) \right) u^7 \\
&+ \frac{8667496367}{34927200} \pi u^{15/2} \\
&+ \left(\frac{54784}{105} \gamma \ln(u) + \frac{219136}{105} \ln(2)^2 - \frac{147087852683}{17463600} \ln(2) + \frac{54784}{105} \gamma^2 + \frac{219136}{105} \ln(2) \gamma - \frac{148697438501}{30965760} \pi^2 \right. \\
&\quad \left. - \frac{2203104637}{33554432} \pi^4 - \frac{9765625}{38016} \ln(5) + \frac{109568}{105} \ln(2) \ln(u) - \frac{98943259619}{17463600} \gamma - \frac{98943259619}{34927200} \ln(u) \right. \\
&\quad \left. + \frac{13696}{105} \ln(u)^2 - \frac{5875497}{4928} \ln(3) + \frac{531841058042717}{9779616000} - 1024\zeta(3) \right) u^8 \\
&+ \frac{87641066621}{209563200} \pi u^{17/2} + O_{\ln}(u^9), \tag{3.21}
\end{aligned}$$

$$\begin{aligned}
g_{S*}^{1\text{SF}^2}(u) = & -\frac{9}{4} - \frac{9}{4}u - \frac{717}{32}u^2 \\
& + \left(\frac{1447441}{960} - \frac{4829}{256}\pi^2 - \frac{16038}{5}\ln(3) + \frac{46976}{15}\ln(2) - \frac{512}{5}\gamma - \frac{256}{5}\ln(u) \right) u^3 \\
& + \left(-\frac{184655453}{38400} + \frac{19162}{35}\gamma + \frac{2097479}{8192}\pi^2 + \frac{454167}{20}\ln(3) - \frac{1081966}{35}\ln(2) + \frac{9581}{35}\ln(u) \right) u^4 \\
& - \frac{714653}{3150}\pi u^{9/2} \\
& + \left(\frac{1136089}{210}\gamma - \frac{19531250}{567}\ln(5) - \frac{82368981}{560}\ln(3) + \frac{121254173}{378}\ln(2) + \frac{1322959637}{196608}\pi^2 + \frac{21119805}{524288}\pi^4 \right. \\
& \quad \left. - \frac{2157036100969787}{26604864000} + \frac{1136089}{420}\ln(u) \right) u^5 \\
& + \frac{214163953}{100800}\pi u^{11/2} \\
& + \left[-9024\zeta(3) - \frac{62597340649}{485100}\gamma + \frac{129552734375}{266112}\ln(5) - \frac{695576369871}{1232000}\ln(3) - \frac{640198452653}{661500}\ln(2) \right. \\
& \quad \left. - \frac{126056977883647}{4459069440}\pi^2 + \frac{549062083551}{167772160}\pi^4 - \frac{149101504}{1575}\gamma\ln(2) + \frac{2808108}{25}\ln(3)\ln(2) + \frac{2808108}{25}\ln(3)\gamma \right. \\
& \quad \left. - \frac{79378592}{525}\ln(2)^2 + \frac{160928}{35}\gamma^2 + \frac{1404054}{25}\ln(3)^2 + \frac{357317643875067280292753}{1035737850115584000} \right. \\
& \quad \left. + \left(-\frac{74550752}{1575}\ln(2) + \frac{1404054}{25}\ln(3) + \frac{160928}{35}\gamma - \frac{62597340649}{970200} \right) \ln(u) + \frac{40232}{35}\ln(u)^2 \right] u^6 \\
& + \frac{193000744063}{93139200}\pi u^{13/2} \\
& + \left[\frac{7394848}{35}\zeta(3) - \frac{4747561509943}{15444000}\ln(7) + \frac{16112853388177387}{15891876000}\gamma - \frac{29717454296875}{8805888}\ln(5) \right. \\
& \quad \left. + \frac{2141915038593471}{448448000}\ln(3) + \frac{5373188171264357}{2270268000}\ln(2) + \frac{36023768285157071}{208089907200}\pi^2 - \frac{9570352156443723}{10737418240}\pi^4 \right. \\
& \quad \left. + \frac{448804392116006600471071523}{5192955612149760000} + \frac{45230944}{63}\gamma\ln(2) - \frac{23385591}{25}\ln(3)\ln(2) - \frac{23385591}{25}\ln(3)\gamma \right. \\
& \quad \left. + \frac{19919007824}{11025}\ln(2)^2 - \frac{1722628912}{11025}\gamma^2 - \frac{23385591}{50}\ln(3)^2 \right. \\
& \quad \left. + \left(\frac{16069729193463787}{31783752000} - \frac{1722628912}{11025}\gamma - \frac{23385591}{50}\ln(3) + \frac{22615472}{63}\ln(2) \right) \ln(u) \right. \\
& \quad \left. - \frac{430657228}{11025}\ln(u)^2 \right] u^7 + O_{\ln}(u^{7.5}), \tag{3.22}
\end{aligned}$$

and

$$g_{S*}^{1\text{SF}^4}(u) = \frac{5}{2} + O(u). \tag{3.23}$$

In these expressions $O_{\ln}(u^n)$ denotes an error term of order u^n modulo a coefficient depending on $\ln u$.

IV. CONVERGENCE OF THE PN-EXPANDED SPIN-ORBIT FUNCTIONS, AND COMPARISON TO NUMERICAL SF DATA

As was pointed out in many previous works (notably Refs. [31, 35, 36]), the speed of convergence of PN expansions is essentially determined by the distance between

the origin and the first expected singularity of the corresponding exact function. For instance, the fact that the 1SF contribution, $a_{1\text{SF}}(u)$, to the EOB $A(u; \nu)$ potential ($A(u; \nu) = 1 - 2u + \nu a_{1\text{SF}}(u) + O(\nu^2)$) has its first singularity at the lightring (LR) [37], $a_{1\text{SF}}(u) \sim (1 - 3u)^{-1/2}$, suggests that the n th term in the PN expansion¹ $a_{1\text{SF}}(u)$ is roughly of order $\sim (3u)^n$, and that the remainder after the n th term is roughly of order $\sim (3u)^{(n+1)} / (1 - 3u)$ [23, 31, 36]. In the present work, we are mainly inter-

¹ We recall that $u = GM/(c^2r)$ so that (modulo the conventional consideration of what low-order term is considered as being “Newtonian”), a term of order u^n is of n PN order.

ested in the PN expansion of the $O(e^2)$ contribution to a SF function of $u_p = 1/p$ and e . In the p, e plane, the *separatrix* of equation $p = 6 + 2e$ (see, e.g., Ref. [38]) marks the boundary between stable and unstable (plunging) eccentric orbits. This boundary (with its attendant change of character of the orbit) is likely to introduce a singularity in generic dynamical functions of p and e . When expanding such functions in powers of e , this will then induce a singularity in the u -dependent coefficients of this expansion at the location $p = 6$, i.e. at the Last Stable (circular) Orbit (LSO), namely, $u_p = u_{\text{LSO}} = 1/6$. For instance, Eq. (5.26) of [39] shows (when using the regularity of the EOB 1SF potentials $a_{1\text{SF}}(u)$ and $d_{1\text{SF}}(u)$ at $u = u_{\text{LSO}} = 1/6$) that the term of order e^2 , say $z_{1\text{SF}}^{(2)}(u_p)$, in the eccentricity expansion of the 1SF contribution to the averaged redshift of particle 1, has a singularity of the form $z_{1\text{SF}}^{(2)}(u_p) \sim (1 - 6u_p)^{-1}$ at $u_p = u_{\text{LSO}} = 1/6$. We similarly expect $\Delta\psi^{(2)}(u_p)$ to have a singularity at $u_p = u_{\text{LSO}} = 1/6$. By the general argument above, this singularity should entail that the n th term in the PN expansion of $\Delta\psi^{(2)}(u_p) = \sum_n C_n^{\psi^{(2)}}(\ln u_p) u_p^n$ has a value, when evaluated at $u_p = u_{\text{LSO}} = 1/6$, that is roughly independent of n , say

$$C_n^{\psi^{(2)}, \text{LSO}} \equiv \left[C_n^{\psi^{(2)}}(\ln u_p) u_p^n \right]_{u_p=\frac{1}{6}} \sim \pm c(\psi^{(2)}), \quad (4.1)$$

where $c(\psi^{(2)})$ is a number of order unity. In turn, this behavior implies that the value of the n th PN term at any u_p is roughly of order

$$C_n^{\psi^{(2)}}(\ln u_p) u_p^n \sim C_n^{\psi^{(2)}, \text{LSO}} (6u_p)^n \sim \pm c(\psi^{(2)}) (6u_p)^n. \quad (4.2)$$

Actually, things might be more subtle than just explained. Indeed, as the SF function $\Delta\psi(u_p, e)$ comes from SF expanding the function $\psi(\Omega_r, \Omega_\phi)$ it might inherit singularities at the other separatrix where the two frequencies Ω_r, Ω_ϕ become degenerate [40, 41], i.e. where the Jacobian $J = \partial(\Omega_r, \Omega_\phi)/\partial(p, e)$ vanishes. Eq. (13) of [41] shows that this occurs when $4p^2 - 39p + 86 = 4p^2(1 - \frac{39}{4}u_p + \frac{43}{2}u_p^2) = 0$. The relevant root is

$$u_{\text{isopairing}} = \frac{1}{172}(39 - \sqrt{145}) \simeq 0.1567349 \simeq \frac{1}{6.380199}. \quad (4.3)$$

For instance, Eq. (2.9) above shows that the zero-eccentricity $\Delta\psi^{(0)}(u_p)$ limit of $\Delta\psi(u_p, e)$ has its first singularity at $u_p = u_{\text{isopairing}} < u_{\text{LSO}}$. However, Eq. (2.9) shows also that there is an extra factor $1 - 6u$ in the numerator of the singular piece in $\Delta\psi^{(0)}(u_p)$, so that one expects PN-expansion coefficients of the rough type $\sim c(u/u_{\text{isopairing}})^n$ with a numerically small prefactor $c \propto 1 - 6u_{\text{isopairing}} \simeq 0.05959$.

In Table I, we list the numerical values of the successive $O_{\ln}(u^n)$ contributions to both $\Delta\psi^{(0)}(u_p)$ and $\Delta\psi^{(2)}(u_p)$,

TABLE I: The numerical values of the successive $O_{\ln}(u^n)$ contributions to both $\Delta\psi^{(0)}(u_p)$ and $\Delta\psi^{(2)}(u_p)$, evaluated at $u = u_{\text{LSO}} = 1/6$. Here, $\eta = \frac{1}{c}$ counts the half-PN orders.

PN	$\Delta\psi^{(0)}(1/6)$	$\Delta\psi^{(2)}(1/6)$
η^2	-0.166667	-
η^4	0.062500	0.027778
η^6	0.126016	+0.076715
η^8	-0.004643	+0.024805
η^{10}	-0.052192	-0.233017
η^{11}	+0.026164	+0.083675
η^{12}	+0.109184	+0.4389648
η^{13}	-0.034307	-0.185439
η^{14}	-0.001642	+0.085211
η^{15}	+0.004381	+0.039424
η^{16}	-0.081211	-0.977197
η^{17}	+0.047979	+0.544810
η^{18}	+0.057535	+0.907178
η^{19}	-0.044808	-
η^{20}	+0.387238 $\times 10^{-3}$	-
η^{21}	-0.196585 $\times 10^{-3}$	-

evaluated at $u = u_{\text{LSO}} = 1/6$. [In the case of $\Delta\psi^{(0)}$, we are neglecting here the (fractionally small) difference between $u_{\text{isopairing}}$ and $\frac{1}{6}$.] The results are compatible with the expectations just explained. In particular, the coefficients $C_n^{\psi^{(2)}, \text{LSO}}$, Eq. (4.1), seem to stabilize at values of order $\sim \pm 1$ as n gets large. [Note that the PN order n takes, after a while, both integer and half-integer values.]

These results allow us to write down a rough theoretical estimate of the remainder of any truncated PN expansion, such as

$$[\Delta\psi^{(2)}(u_p)]^{N \text{PN}}(u) = \sum_{n=2}^N C_n^{\psi^{(2)}}(\ln u_p) u_p^n. \quad (4.4)$$

Namely, one expects the absolute value of the N -PN remainder, $[\Delta\psi^{(2)}(u_p)]^{\text{exact}} - [\Delta\psi^{(2)}(u_p)]^{N \text{PN}}$, to be roughly of order (using the fact that, in the cases we shall consider, the next term differs by a half PN order)

$$\sigma_{N \text{PN}}^{\text{th}}(\Delta\psi^{(2)}(u)) = \left| C_{N+\frac{1}{2}}^{\psi^{(2)}, \text{LSO}} \right| \frac{(6u)^{(N+\frac{1}{2})}}{(1-6u)^{\alpha_N}}. \quad (4.5)$$

Here, like in our previous works [31, 36], we allow for the possibility of having not only an overall numerical prefactor, namely $C_{N+\frac{1}{2}}^{\psi^{(2)}, \text{LSO}}$, but also to correct the contribution of the next, $N + \frac{1}{2}$ th, PN contribution by a u -dependent factor $(1-6u)^{-\alpha_N}$ which resums the missing higher-order PN contributions. In the cases considered in Refs. [31, 36] (which dealt with singularities at the lightning), one had some a priori estimates of the value

of the exponent α_N entering the latter factor. In the cases considered here of singularities at the LSO, we do not have such a priori estimates, and we shall choose the values of the exponent α_N so as to increase the agreement with the numerical SF data to be discussed next.

Ref. [26] has computed numerical values for $\Delta\psi(u_p, e)$ for selected values of $e = [0.05 + 0.25k]_{k=0..8}$ and $u_p = [(10 + 5k)^{-1}]_{k=0..18}$. Then Ref. [25] extracted (by a fitting procedure) from the latter numerical data, secondary numerical data for the function $\Delta\psi^{(2)}(u_p)$ parametrizing the $O(e^2)$ contribution to $\Delta\psi(u_p, e)$. In Ref. [25] the latter numerically-derived values of $\Delta\psi^{(2)}(u_p)$ (corresponding to a discrete sample of values of the u_p 's) were denoted $m^{\text{num}}(u_p)$, and they were completed by an estimate of a corresponding numerical (fitting) error, denoted $\sigma_m^{\text{num}}(u_p)$. In Ref. [25] we had compared the list of numerical data $m^{\text{num}}(u_p) \pm \sigma_m^{\text{num}}(u_p)$ to the 6PN-accurate theoretical expression for $\Delta\psi^{(2)}(u_p)$ that we had derived there. Here, we shall investigate to what extent the improved (9PN-accurate) theoretical expression for $\Delta\psi^{(2)}(u_p)$ derived above improves the agreement between numerical data and theoretical values. Such a comparative study must crucially take into account both the numerical error $\sigma_m^{\text{num}}(u_p)$ and the relevant theoretical error, as estimated by using the general formula (4.5). More precisely, when dealing with the 6PN-accurate result of Ref. [25], as we (now) know the value of the numerical coefficient $C_{6.5}^{\psi^{(2)}, \text{LSO}}$, namely $C_{6.5}^{\psi^{(2)}, \text{LSO}} \approx -0.185439$, we shall use its absolute value in defining $\sigma_{6\text{PN}}^{\text{th}}(\Delta\psi^{(2)}(u))$. In addition, we found that including an extra factor $(1 - 6u)^{-\alpha_6}$, with the exponent $\alpha_6 = 1$, improved the consistency with the numerical data. In other words, we use $\sigma_{6\text{PN}}^{\text{th}}(\Delta\psi^{(2)}(u)) = 0.185439(6u)^{6.5}/(1 - 6u)$. On the other hand, for the a priori estimate of the theoretical error on our new 9PN-accurate expression for $\Delta\psi^{(2)}(u)$, as we do not know the LSO value of the 9.5PN contribution, we simply use as overall numerical coefficient a coefficient equal to 1 (as suggested by the last values in the second column of Table I). In addition, we found that the agreement with numerical data was slightly better when using no additional LSO-blowup factor, i.e. we use $\alpha_9 = 0$. In other words, we simply use $\sigma_{9\text{PN}}^{\text{th}}(\Delta\psi^{(2)}(u)) = (6u)^{9.5}$.

The important thing is then to compare the two different numerical-minus-theoretical discrepancies, say

$$\begin{aligned} \delta^{6\text{PN}}(u_p) &\equiv m^{\text{num}}(u_p) - \Delta\psi^{(2)\text{6PN}}(u_p), \\ \delta^{9\text{PN}}(u_p) &\equiv m^{\text{num}}(u_p) - \Delta\psi^{(2)\text{9PN}}(u_p), \end{aligned} \quad (4.6)$$

to a measure of the total error, combining both the numerical one and the (corresponding) theoretical one. As is standard, we define the two total errors corresponding to the two relevant cases (6PN vs 9PN theoretical accuracies) by summing the two separate errors in quadrature,

namely

$$\begin{aligned} \sigma_{6\text{PN}}^{\text{tot}}(\Delta\psi^{(2)}(u_p)) &\equiv \sqrt{(\sigma_m^{\text{num}}(u_p))^2 + (\sigma_{6\text{PN}}^{\text{th}}(u_p))^2}, \\ \sigma_{9\text{PN}}^{\text{tot}}(\Delta\psi^{(2)}(u_p)) &\equiv \sqrt{(\sigma_m^{\text{num}}(u_p))^2 + (\sigma_{9\text{PN}}^{\text{th}}(u_p))^2}. \end{aligned} \quad (4.7)$$

In Table II we present the values of the two different numerical-minus-theoretical discrepancies (4.6), together with the two corresponding total errors (4.7). The corresponding (discrete) data points are plotted (on a semi-logarithmic scale, and using absolute values) in Fig. 1. In the latter figure, we have also indicated the two continuous curves representing the (base-10 logarithms of the) two theoretical errors (4.5), for $N = 6$ and $N = 9$. Note that each (absolute) value of $\delta^{N\text{PN}}(u_p)$ is quite close to the corresponding total error $\sigma_{N\text{PN}}^{\text{tot}}$. More precisely, for $u_p \leq 0.0154$ (i.e. $p \geq 65$) the four different values $\delta^{6\text{PN}}(u_p)$, $\delta^{9\text{PN}}(u_p)$, $\sigma_{6\text{PN}}^{\text{tot}}$, $\sigma_{9\text{PN}}^{\text{tot}}$, are all close to each other, because the theoretical estimates are much closer to each other than the numerical error, and because they are also in agreement with the numerical data (within the numerical error). On the other hand, for $u_p > 0.0154$, the data points corresponding to each separate PN accuracy (6PN vs 9PN) are still close to each other (showing the consistency, modulo the total error, of each theoretical estimate with the numerical data), but there is now a notable vertical distance between $(|\delta^{6\text{PN}}(u_p)|, \sigma_{6\text{PN}}^{\text{tot}})$, on one side, and, $(|\delta^{9\text{PN}}(u_p)|, \sigma_{9\text{PN}}^{\text{tot}})$, on the other side. For this part of the plot, the total error is dominated by the corresponding theoretical one, and we see that the improved theoretical accuracy is effective in bringing an improved agreement with the numerical data. This brings a direct numerical confirmation of our new theoretical results.

The analysis above has provided us with an estimate of the theoretical error on our new, 9PN-accurate result for $\Delta\psi^{(2)}(u_p)$, namely the function $\sigma_{9\text{PN}}^{\text{th}}(\Delta\psi^{(2)}(u)) = (6u)^{9.5}$. This theoretical error gets large as u approaches $\frac{1}{6}$. More precisely, one finds that the fractional theoretical error

$$\frac{\sigma_{9\text{PN}}^{\text{th}}(\Delta\psi^{(2)}(u))}{\Delta\psi^{(2)\text{9PN}}(u)} \quad (4.8)$$

increases monotonically with u , to reach 12.4% when $u = 0.09$, 22.7% when $u = 0.1$, and 36.7% when $u = 0.11$. This illustrates again the poor convergence of PN approximants. Here, the situation is worse than usual because, as we argued above, the function $\Delta\psi^{(2)}(u)$ probably has a singularity at (or near) $u = u_{\text{LSO}} = \frac{1}{6} = 0.1666\dots$. Even our 9PN-accurate expansion becomes useless above $u \simeq 0.1$.

In Fig. 2, left panel, we plot the sequence of N -PN approximants to $\Delta\psi^{(2)}(u)$, as defined in Eq. (4.4), for $N \geq 3$. In the right panel, instead we compare our 9PN result for $\Delta\psi^{(2)}(u)$ to the numerical data extracted from Ref. [26].

TABLE II: We compare the two theoretical values $m_i^{\text{thy}} \equiv \Delta\psi^{(2)\text{PN}}(p_i)$ at 6PN (Ref. [25]) and 9PN (this work) and the corresponding numerical-minus-theoretical discrepancies δ_i defined in Eq. (4.6). The estimates of the corresponding uncertainties in their values are indicated in parenthesis. The second column shows the numerical estimates m_i^{num} obtained in Ref. [25] by least-squares fitting the numerical data for $\Delta\psi(p, e)$ given in Ref. [26].

p	$m^{\text{num}}(\sigma_m^{\text{num}}) _{\text{Ref.}[25]}$	$m^{\text{thy}}(\sigma_m^{\text{thy}}) _{6\text{PN}}$	$\delta^{6\text{PN}}(\sigma_m^{\text{tot}})$	$m^{\text{thy}}(\sigma_m^{\text{thy}}) _{9\text{PN}}$	$\delta^{9\text{PN}}(\sigma_m^{\text{tot}})$
10	$2.83892(11) \times 10^{-2}$	$3.9(1.7) \times 10^{-2}$	$-0.11(17) \times 10^{-1}$	$3.44(78) \times 10^{-2}$	$-0.060(78) \times 10^{-1}$
15	$9.12787(61) \times 10^{-3}$	$9.99(80) \times 10^{-3}$	$-8.6(8.0) \times 10^{-4}$	$9.28(17) \times 10^{-3}$	$-0.16(16) \times 10^{-3}$
20	$4.40237(32) \times 10^{-3}$	$4.54(11) \times 10^{-3}$	$-1.4(1.1) \times 10^{-4}$	$4.415(11) \times 10^{-3}$	$-0.13(11) \times 10^{-4}$
25	$2.561664(35) \times 10^{-3}$	$2.596(23) \times 10^{-3}$	$-3.5(2.3) \times 10^{-5}$	$2.5640(13) \times 10^{-3}$	$-0.23(13) \times 10^{-5}$
30	$1.66508(23) \times 10^{-3}$	$1.6765(66) \times 10^{-3}$	$-1.14(66) \times 10^{-5}$	$1.66632(23) \times 10^{-3}$	$-0.123(33) \times 10^{-5}$
35	$1.16553(20) \times 10^{-3}$	$1.1697(24) \times 10^{-3}$	$-4.1(2.4) \times 10^{-6}$	$1.165845(53) \times 10^{-3}$	$-3.2(2.1) \times 10^{-7}$
40	$8.5943(13) \times 10^{-4}$	$8.6114(96) \times 10^{-4}$	$-1.71(97) \times 10^{-6}$	$8.59511(15) \times 10^{-4}$	$-0.86(13) \times 10^{-7}$
45	$6.58803(62) \times 10^{-4}$	$6.5969(44) \times 10^{-4}$	$-8.8(4.4) \times 10^{-7}$	$6.589218(49) \times 10^{-4}$	$-1.20(62) \times 10^{-7}$
50	$5.20356(82) \times 10^{-4}$	$5.2107(22) \times 10^{-4}$	$-7.1(2.3) \times 10^{-7}$	$5.206806(18) \times 10^{-4}$	$-3.25(82) \times 10^{-7}$
55	$4.2124(14) \times 10^{-4}$	$4.2171(12) \times 10^{-4}$	$-4.8(1.8) \times 10^{-7}$	$4.2150318(72) \times 10^{-4}$	$-2.7(1.4) \times 10^{-7}$
60	$3.4798(15) \times 10^{-4}$	$3.48128(65) \times 10^{-4}$	$-1.5(1.6) \times 10^{-7}$	$3.4800907(32) \times 10^{-4}$	$-0.3(1.5) \times 10^{-7}$
65	$2.9178(37) \times 10^{-4}$	$2.92146(38) \times 10^{-4}$	$-3.6(3.7) \times 10^{-7}$	$2.9207548(15) \times 10^{-4}$	$-2.9(3.7) \times 10^{-7}$
70	$2.4793(43) \times 10^{-4}$	$2.48589(24) \times 10^{-4}$	$-6.6(4.3) \times 10^{-7}$	$2.48544960(73) \times 10^{-4}$	$-6.2(4.3) \times 10^{-7}$
75	$2.1347(49) \times 10^{-4}$	$2.14046(15) \times 10^{-4}$	$-5.7(4.9) \times 10^{-7}$	$2.14017950(38) \times 10^{-4}$	$-5.4(4.9) \times 10^{-7}$
80	$1.8583(90) \times 10^{-4}$	$1.861997(98) \times 10^{-4}$	$-3.7(9.0) \times 10^{-7}$	$1.86181379(21) \times 10^{-4}$	$-3.5(9.0) \times 10^{-7}$
85	$1.6289(97) \times 10^{-4}$	$1.634304(66) \times 10^{-4}$	$-5.4(9.7) \times 10^{-7}$	$1.63417981(12) \times 10^{-4}$	$-5.3(9.7) \times 10^{-7}$
90	$1.4552(39) \times 10^{-4}$	$1.445785(45) \times 10^{-4}$	$+9.5(3.9) \times 10^{-7}$	$1.445699417(67) \times 10^{-4}$	$+9.5(3.9) \times 10^{-7}$
95	$1.292(10) \times 10^{-4}$	$1.287970(32) \times 10^{-4}$	$+0.4(1.0) \times 10^{-6}$	$1.287910310(40) \times 10^{-4}$	$+0.4(1.0) \times 10^{-6}$
100	$1.130(14) \times 10^{-4}$	$1.154556(23) \times 10^{-4}$	$-2.4(1.4) \times 10^{-6}$	$1.154513310(25) \times 10^{-4}$	$-2.4(1.4) \times 10^{-6}$

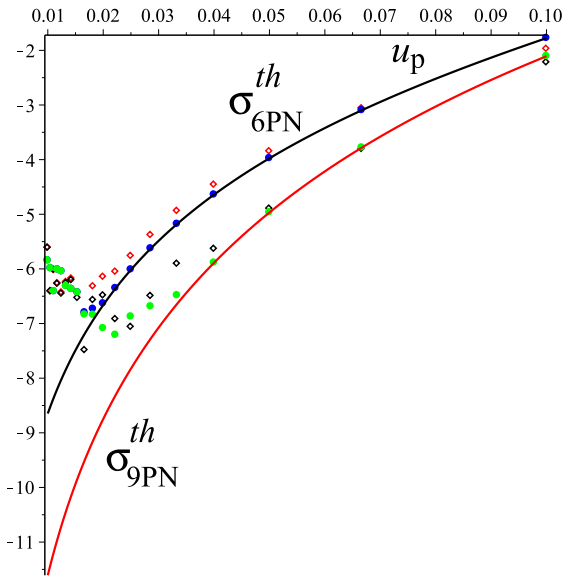


FIG. 1: The data points associated with $\delta^{6\text{PN}}(u_p)$ (diamonds, red online), $\delta^{9\text{PN}}(u_p)$ (diamonds, black online), $\sigma_{6\text{PN}}^{\text{tot}}$ (solid circles, blue online), $\sigma_{9\text{PN}}^{\text{tot}}$ (solid circles, green online) are plotted on a semi-logarithmic scale as functions of u_p . The two solid curves correspond to (the \log_{10} of) $\sigma_{6\text{PN}}^{\text{th}} = 0.185439(6u_p)^{6.5}/(1-6u_p)$ and $\sigma_{9\text{PN}}^{\text{th}} = (6u_p)^{9.5}$.

As there are no numerical data for $u_p > 0.1$, and as the current theoretical estimates get (as explained above) completely unreliable for $u_p > 0.1$, we see that we have no firm knowledge of the behavior of $\Delta\psi^{(2)}(u)$ for $u_p \gtrsim 0.1$. The enormous spread among the various PN approximants cannot reliably tell us whether $\Delta\psi^{(2)}(u)$ goes to $+\infty$ or $-\infty$ (or has a milder behavior) as u approaches $\frac{1}{6}$.

Finally, let us discuss the convergence properties of the PN expansion of the 1SF contributions to the EOB gyrogravitomagnetic ratio $g_{S*}(u, p_r, p_\phi, \nu)$. We recall that, according to Eq. (3.12), the SF expansion (i.e. the expansion in powers of ν) of $g_{S*}(u, p_r, p_\phi, \nu)$ is decomposed into the zeroth contribution (3.13) (expressed as a specific function of u , p_r and p_ϕ), and into a 1SF contribution (3.15) which is expanded in powers of p_r^2 . Here, we expect different radii of convergence for the PN expansions of the various contributions $g_{S*}^{1\text{SF}0}(u)$, $g_{S*}^{1\text{SF}2}(u)$, ... to the 1SF term $g_{S*}^{(\nu^1)}(u, p_r)$. Indeed, when taking from the start the limit $p_r \rightarrow 0$, i.e., when considering the sequence of circular orbits, the only place where a singularity can appear is at the LR, i.e., for $u = u_{\text{LR}} = \frac{1}{3}$. We then expect that the successive PN terms in the PN expansion of the function $g_{S*}^{1\text{SF}0}(u)$ will be of order 1 at $u = u_{\text{LR}} = \frac{1}{3}$. The first column of Table III lists the separate, successive PN contributions to $g_{S*}^{1\text{SF}0}(u)$, evaluated at $u = \frac{1}{3}$, and we

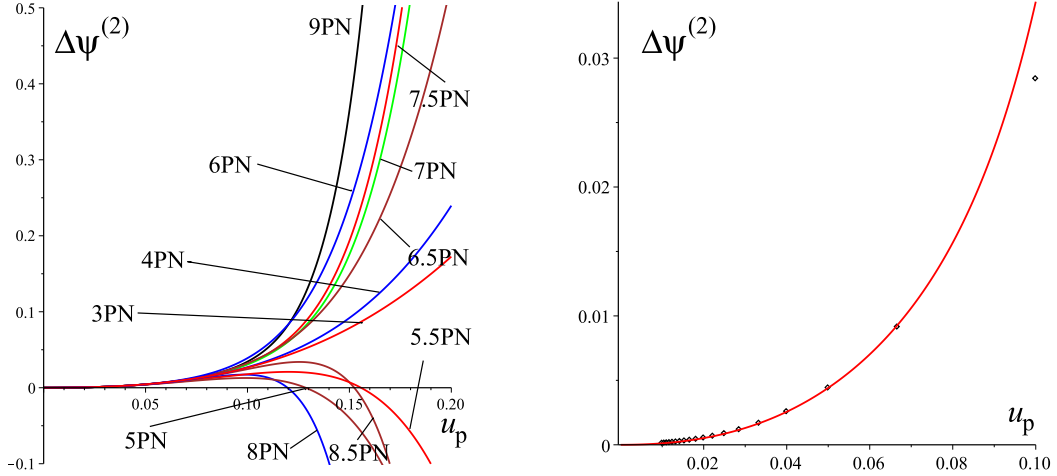


FIG. 2: (Left panel) The various PN-approximants to $\Delta\psi^{(2)}(u_p)$, Eq. (4.4) with $3 \leq N \leq 9$, are plotted as functions of the inverse-semilatus rectum u_p . (Right panel) Our 9PN result for $\Delta\psi^{(2)}(u_p)$ superposed to the corresponding data extracted (in Ref. [25]) from Ref. [26].

see that, indeed, they are roughly all of order unity.

On the other hand, because of the specific gauge choice we made of writing (for definiteness) the coefficient $g_{S^*}^{1\text{SF}2}(u)$ of the $O(p_r^2)$ contribution to $g_{S^*}^{(\nu^1)}(u, p_r)$ as a function only of u (rather than of both u and p_ϕ), it is to be expected that the function $g_{S^*}^{1\text{SF}2}(u)$ will inherit from its “source” function $\Delta\psi^{(2)}(u_p)$ the presence of a singularity at the LSO, i.e. at $u = u_{\text{LSO}} = \frac{1}{6}$. Indeed, even if we assume the existence of some unknown EOB function $g_{S^*}^{(\nu^1)}(u, p_r, p_\phi)$ that would hopefully only be singular at the LR (but be regular at the LSO), one needs to apply a gauge transformation to gauge-fix $g_{S^*}^{(\nu^1)}(u, p_r, p_\phi)$ into the form $g_{S^*}^{(\nu^1)}(u, p_r)$, and the determination of this transformation must involve the comparison of gauge-invariant functions of two variables, i.e., functions of the two frequencies Ω_r and Ω_ϕ . For the reasons explained above, the latter comparison will then introduce an extra singularity at $u = u_{\text{LSO}} = \frac{1}{6}$. In the second column of Table III we list the separate, successive PN contributions to $g_{S^*}^{1\text{SF}2}(u)$, evaluated at $u = \frac{1}{6}$, and we see that, indeed, they stay roughly all of order unity (possibly except for the last one, which is largish). By contrast, when evaluating the successive PN contributions to $g_{S^*}^{1\text{SF}2}(u)$, evaluated at $u = \frac{1}{3}$, we found that they became increasingly large as the PN order increases (for instance the $O(u^6)$ contribution is equal to -75.38253 at $u = \frac{1}{3}$, while the $O(u^7)$ one is equal to 928.63276).

Using the same reasoning we employed above to estimate the theoretical error on the truncated PN expansions of $\Delta\psi^{(2)}(u)$, we then expect that a reasonable estimate of the theoretical error on the current 7PN-accurate PN expansion of $g_{S^*}^{1\text{SF}2}(u)$, Eq. (3.22), i.e., an estimate of the error term $O_{\ln}(u^{7.5})$ in the latter equation, is roughly given by

$$\sigma_{7\text{PN}}^{\text{th}}(g_{S^*}^{1\text{SF}2}(u)) = (6u)^{7.5} / (1 - 6u). \quad (4.9)$$

TABLE III: Numerical values of the successive $O_{\ln}(u^n)$ contributions to both $g_{S^*}^{1\text{SF}0}(u_p)$ (evaluated at $u = u_{\text{LR}} = 1/3$), and $g_{S^*}^{1\text{SF}2}(u_p)$ (evaluated at $u = u_{\text{LSO}} = 1/6$).

PN	$g_{S^*}^{1\text{SF}0}(1/3)$	$g_{S^*}^{1\text{SF}2}(1/6)$
η^0	-	-2.25
η^2	-0.25	-0.375
η^4	-1.083333	-0.622396
η^6	-1.072353	$+0.487256 \times 10^{-2}$
η^8	-0.421860	$+0.820994$
η^9	-	-0.224519
η^{10}	$+0.748491$	-0.919538
η^{11}	-0.442184	$+0.350432$
η^{12}	-2.099104	-0.638599
η^{13}	$+0.775711$	$+0.569630 \times 10^{-1}$
η^{14}	-1.520959	$+6.602989$

The latter error goes to infinity when u approaches $\frac{1}{6} = 0.1666\dots$, and becomes already unacceptably large around $u \simeq 0.13$. Indeed, the (absolute value of the) fractional error $\sigma_{7\text{PN}}^{\text{th}}(g_{S^*}^{1\text{SF}2}(u)) / g_{S^*,7\text{PN}}^{1\text{SF}2}(u)$ increases with u and is found to be equal to 13.68% when $u = 0.12$, and 38.00% when $u = 0.13$. In other words, even the much improved 7PN-accurate expansion of $g_{S^*}^{1\text{SF}2}(u)$ derived in the present work becomes totally unreliable for $u > 0.12$, so that we do not have any solid knowledge of the strong-field behavior of $g_{S^*}^{1\text{SF}2}(u)$. In absence of direct numerical data on $g_{S^*}^{1\text{SF}2}(u)$ we have no firm knowledge of the behavior of this function beyond $u = 0.12$, and, in particular, of its probable singularity structure at $u = \frac{1}{6}$. One would need an analytical knowledge of the latter singularity structure in order to concoct a more regular

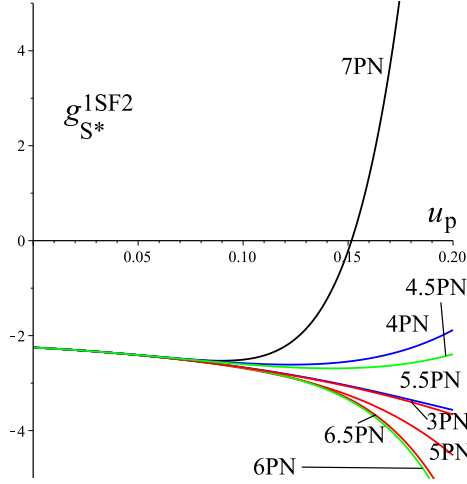


FIG. 3: The various PN-approximants to $g_{S*}^{1SF2}(u_p)$, Eq. (3.22), are plotted as functions of the inverse-semilatus rectum u_p .

version, say $g_{S*}^{1SF2}(u, p_\phi)$, involving some dependence on p_ϕ . The enormous strong-field spread among the various PN approximants to $g_{S*}^{1SF2}(u)$ is illustrated in Fig. 3.

V. CONCLUDING REMARKS

Improving upon recent results by Kavanagh et al. [25], we have analytically computed, through the ninth post-Newtonian (PN) order, the $O(e^2)$ contribution to the (first-order) gravitational self-force (SF) correction to the spin-orbit precession of a spinning compact body along a slightly eccentric orbit around a Schwarzschild black hole (see Eq. (2.8)). We have then translated this information into its corresponding Effective-One-Body (EOB) counterpart, thereby determining through the (fractional) seventh PN order the $O(p_r^2)$ self-force contribution to the EOB gyrogravitomagnetic ratio g_{S*} (see Eq. (3.22)). We have shown the compatibility between our improved analytical knowledge of $\Delta\psi^{(2)}(u)$ and numerical SF data extracted in Ref. [25] from the numerical results of Ref. [26] (see Fig. 1 and Table II). We have studied the convergence of the PN expansions of both $\Delta\psi^{(2)}(u)$ and $g_{S*}^{1SF2}(u)$ and emphasized that their convergence is much worse than that of the usual, circular-orbit related dynamical quantities. Indeed, the existence, in the unperturbed background spacetime, of a Last Stable (circular) Orbit (LSO) at $r = 6GM/c^2$ implies the presence of a singularity at $u = \frac{1}{6}$ in the (exact) functions $\Delta\psi^{(2)}(u)$ and $g_{S*}^{1SF2}(u)$, and, this singularity then entails that the radius of convergence of the PN expansions of $\Delta\psi^{(2)}(u)$ and $g_{S*}^{1SF2}(u)$ is only equal to $u_{LSO} = \frac{1}{6}$. This radius of convergence is twice smaller than that of the usual, circular-orbit related dynamical potentials (such as the SF contribution $a_{1SF}(u)$ to the main EOB radial potential). The resulting bad convergence of the sequence of

PN approximants has been illustrated in Figs. 2 and 3. If one wants to overcome this problem, one would need to study the precise analytical structure of the LSO singularity of the functions $\Delta\psi^{(2)}(u)$ and $g_{S*}^{1SF2}(u)$. We leave this task to future work, as well as the technically challenging task of further extending our results in the following directions: computing higher PN orders, including higher order contributions in eccentricity, and taking into account the spin of the central black hole.

Appendix A: Definition of the spin-precession invariant

1. Gyroscope precession in the background spacetime

The tangent 4-velocity \bar{u} ($\bar{u} \cdot \bar{u} = -1$) to an unperturbed eccentric geodesic orbit on the equatorial plane of the background Schwarzschild spacetime is given by

$$\bar{u} = \bar{u}^\alpha \partial_\alpha = \frac{\bar{E}}{f} \partial_t + \dot{r} \partial_r + \frac{\bar{L}}{r^2} \partial_\phi, \quad (\text{A1})$$

where $\dot{r} \equiv \bar{u}^r$ is such that

$$\dot{r}^2 = \left(\frac{dr}{d\bar{\tau}} \right)^2 = \bar{E}^2 - f \left(1 + \frac{\bar{L}^2}{r^2} \right). \quad (\text{A2})$$

The orbit can be parametrized either by the proper time $\bar{\tau}$ or by the relativistic anomaly $\chi \in [0, 2\pi]$, such that

$$r = \frac{m_2 p}{1 + e \cos \chi}. \quad (\text{A3})$$

They are related by

$$\frac{d\bar{\tau}}{d\chi} = \frac{m_2 p^{3/2}}{(1 + e \cos \chi)^2} \left[\frac{p - 3 - e^2}{p - 6 - 2e \cos \chi} \right]^{1/2}. \quad (\text{A4})$$

The (dimensionless) background orbital parameters, semi-latus rectum p and eccentricity e , are defined by writing the minimum (pericenter, r_{peri}) and maximum (apocenter, r_{apo}) values of the (areal) radial coordinate along the orbit as

$$r_{\text{peri}} = \frac{m_2 p}{1 + e}, \quad r_{\text{apo}} = \frac{m_2 p}{1 - e}. \quad (\text{A5})$$

They are in correspondence with the conserved (dimensionless) energy $\bar{E} = -\bar{u}_t$ and angular momentum $\bar{L} = \bar{u}_\phi$ per unit mass of the particle, via

$$\bar{E}^2 = \frac{(p - 2)^2 - 4e^2}{p(p - 3 - e^2)}, \quad \bar{L}^2 = \frac{p^2}{p - 3 - e^2}. \quad (\text{A6})$$

The reciprocal of p , $u_p \equiv p^{-1}$, is a useful argument, which serves also as PN expansion parameter.

Eq. (A4) can be used to solve the equations for t and ϕ as functions of χ , which are then solvable in terms of elliptic functions. As is well known, eccentric orbits

are characterized by two fundamental frequencies, $\bar{\Omega}_r = 2\pi/\bar{T}_r$ and $\bar{\Omega}_\phi = \bar{\Phi}/\bar{T}_r$, where $\bar{\Phi} = \oint d\phi = \oint d\chi d\phi/d\chi$ is the angular advance during one radial period, $\bar{T}_r = \oint dt = \oint d\chi dt/d\chi$. To second order in e we find

$$\begin{aligned} m_2 \bar{\Omega}_r &= u_p^{3/2} (1 - 6u_p)^{1/2} \left[1 - \frac{3}{4} \frac{2 - 32u_p + 165u_p^2 - 266u_p^3}{(1 - 2u_p)(1 - 6u_p)^2} e^2 + O(e^4) \right], \\ m_2 \bar{\Omega}_\phi &= u_p^{3/2} \left[1 - \frac{3}{2} \frac{1 - 10u_p + 22u_p^2}{(1 - 2u_p)(1 - 6u_p)} e^2 + O(e^4) \right]. \end{aligned} \quad (\text{A7})$$

The gyroscope precession is defined with respect to the Marck-type frame [42] adapted to \bar{u} , completed by the spatial triad

$$\begin{aligned} \bar{e}_1 &= \frac{1}{\sqrt{1 + \bar{L}^2/r^2}} \left[\frac{\dot{r}}{f} \partial_t + \bar{E} \partial_r \right], \\ \bar{e}_2 &= \frac{1}{r} \partial_\theta, \\ \bar{e}_3 &= \frac{1}{\sqrt{1 + \bar{L}^2/r^2}} \left[\frac{\bar{L}}{r} \bar{u} + \frac{1}{r} \partial_\phi \right], \end{aligned} \quad (\text{A8})$$

whose transport properties are

$$\nabla_{\bar{u}} \bar{e}_1 = \bar{\omega} \bar{e}_3, \quad \nabla_{\bar{u}} \bar{e}_3 = -\bar{\omega} \bar{e}_1, \quad (\text{A9})$$

with

$$\bar{\omega} = \frac{\bar{E} \bar{L}}{r^2 + \bar{L}^2}. \quad (\text{A10})$$

The precession angle of a test gyroscope dragged along \bar{u} is then given by

$$\bar{\psi} = 1 - \frac{\bar{\Psi}}{\bar{\Phi}}, \quad (\text{A11})$$

where

$$\bar{\Psi} = \int_0^{\bar{\tau}} \bar{\omega} d\bar{\tau} = \int_0^{2\pi} \bar{\omega} \frac{d\bar{\tau}}{d\chi} d\chi, \quad (\text{A12})$$

which finally yields

$$\begin{aligned} \bar{\psi} &= 1 - \sqrt{1 - 3u_p} \\ &+ \frac{3}{2} \frac{(1 - 4u_p)u_p^2}{(1 - 2u_p)(1 - 6u_p)\sqrt{1 - 3u_p}} e^2 \\ &+ O(e^4). \end{aligned} \quad (\text{A13})$$

2. Spin precession in the perturbed spacetime

Bound timelike geodesics in the equatorial plane of the perturbed spacetime have 4-velocity

$$\begin{aligned} u &= u^\alpha \partial_\alpha = (\bar{u}^\alpha + \delta u^\alpha) \partial_\alpha \\ &= \frac{1}{f} (\bar{E} + \delta E) \partial_t + (\bar{u}^r + \delta u^r) \partial_r + \frac{1}{r^2} (\bar{L} + \delta L) \partial_\phi, \end{aligned} \quad (\text{A14})$$

with $\delta u^\alpha = O(h)$. Here, δu^r follows from the normalization condition of u with respect to the perturbed metric, which reads

$$\bar{u}^r \delta u^r = \bar{E} \delta E - \frac{\bar{L}}{r^2} f \delta L - \frac{1}{2} f h_{00}, \quad (\text{A15})$$

where $h_{00} = h_{\alpha\beta} \bar{u}^\alpha \bar{u}^\beta$. Equivalently, one can normalize u with respect to the background metric as in Barack and Sago (BS) [40], leading to

$$\bar{u}^r \delta u_{BS}^r = \bar{E} \delta E_{BS} - \frac{\bar{L}}{r^2} f \delta L_{BS}, \quad (\text{A16})$$

where

$$\begin{aligned} \delta E_{BS} &= \delta E - \frac{1}{2} \bar{E} h_{00}, \\ \delta u_{BS}^r &= \delta u^r - \frac{1}{2} \bar{u}^r h_{00}, \\ \delta L_{BS} &= \delta L - \frac{1}{2} \bar{L} h_{00}. \end{aligned} \quad (\text{A17})$$

The 4-velocity 1-form turns out to be

$$\begin{aligned} u^\flat &= u_\alpha dx^\alpha \\ &= -(\bar{E} + \delta E - h_{t\bar{u}}) dt + \frac{1}{f} (\dot{r} + \delta u^r + f h_{r\bar{u}}) dr \\ &\quad + (\bar{L} + \delta L + h_{\phi\bar{u}}) d\phi, \end{aligned} \quad (\text{A18})$$

where $h_{\alpha\bar{u}} = h_{\alpha\beta} \bar{u}^\beta$, and where the further equatorial plane condition $\delta u_\theta = 0$ (implying $h_{\theta\bar{u}} = 0$) has been assumed.

The geodesic equations

$$\frac{du_\alpha}{d\tau} - \frac{1}{2} (\bar{g}_{\lambda\mu,\alpha} + h_{\lambda\mu,\alpha}) u^\lambda u^\mu = 0, \quad (\text{A19})$$

determine the evolution of δu_t and δu_ϕ , or equivalently of the perturbations in energy δE and angular momentum δL by

$$\begin{aligned} \frac{d}{d\tau} \delta E &= \frac{1}{2} \bar{E} \frac{dh_{00}}{d\tau} - F_t, \\ \frac{d}{d\tau} \delta L &= \frac{1}{2} \bar{L} \frac{dh_{00}}{d\tau} + F_\phi, \end{aligned} \quad (\text{A20})$$

where the functions F_t and F_ϕ are the covariant t and ϕ components of the self force

$$F^\mu = -\frac{1}{2} (\bar{g}^{\mu\nu} + \bar{u}^\mu \bar{u}^\nu) \bar{u}^\lambda \bar{u}^\rho (2h_{\nu\lambda;\rho} - h_{\lambda\rho;\nu}). \quad (\text{A21})$$

Here we are interested in conservative effects only, i.e., we assume that $F^\alpha = F_{\text{cons}}^\alpha$ results in a periodic function of χ . Eqs. (A20) can then be formally integrated as

$$\begin{aligned} \delta E_{BS}(\chi) &= - \int_0^\chi F_t^{\text{cons}}(\chi) \frac{d\tau}{d\chi} d\chi + \delta E_{BS}(0) \\ &\equiv \mathcal{E}_{BS}(\chi) + \delta E_{BS}(0), \\ \delta L_{BS}(\chi) &= \int_0^\chi F_\phi^{\text{cons}}(\chi) \frac{d\tau}{d\chi} d\chi + \delta L_{BS}(0) \\ &\equiv \mathcal{L}_{BS}(\chi) + \delta L_{BS}(0), \end{aligned} \quad (\text{A22})$$

recalling the relations (A17). Here, the conservative self force components are defined by $F_t^{\text{cons}} = [F_t(\chi) - F_t(-\chi)]/2$ and $F_\phi^{\text{cons}} = [F_\phi(\chi) - F_\phi(-\chi)]/2$. The integration constants $\delta E_{BS}(0)$ and $\delta L_{BS}(0)$ are computed as indicated in Ref. [40], and turn out to be

$$\begin{aligned}\delta E_{BS}(0) &= \frac{(1+e)^2(p-2-2e)}{4e(p-3-e^2)} \times \\ &\quad [(1-e)^2(p-2+2e)B\mathcal{L}_{BS}(\pi) - \mathcal{E}_{BS}(\pi)], \\ \delta L_{BS}(0) &= \frac{1}{4e(p-3-e^2)B} \times \\ &\quad [(1-e)^2(p-2+2e)B\mathcal{L}_{BS}(\pi) - \mathcal{E}_{BS}(\pi)],\end{aligned}\quad (\text{A23})$$

with

$$B = \frac{1}{m_2^2 p^3} \frac{\bar{L}}{\bar{E}} = \frac{1}{m_2 p^{3/2} [(p-2)^2 - 4e^2]^{1/2}}. \quad (\text{A24})$$

The spin precession has been calculated by Akcay et al. [26] with respect to a suitably defined perturbed Marck-type frame $\{u, e_a\}$ adapted to u , with $e_a^\alpha = \bar{e}_a^\alpha + \delta e_a^\alpha$. The first-order SF correction to the spin precession invariant turns out to be given by

$$\Delta\psi = -\frac{\Delta\Psi}{\bar{\Phi}}, \quad (\text{A25})$$

where

$$\Delta\Psi = \delta\Psi - \frac{\partial\bar{\Psi}}{\partial\bar{\Omega}_r}\delta\Omega_r - \frac{\partial\bar{\Psi}}{\partial\bar{\Omega}_\phi}\delta\Omega_\phi. \quad (\text{A26})$$

The SF corrections to the frequencies are given by

$$\delta\Omega_r = -\bar{\Omega}_r \frac{\delta T}{\bar{T}}, \quad \delta\Omega_\phi = -\bar{\Omega}_\phi \left(-\frac{\delta\Phi}{\bar{\Phi}} + \frac{\delta T}{\bar{T}} \right), \quad (\text{A27})$$

where

$$\begin{aligned}\delta T &= \int_0^{2\pi} \left(\frac{\delta u^t}{\bar{u}^t} - \frac{\delta u^r}{\bar{u}^r} \right) \bar{u}^t \frac{d\bar{\tau}}{d\chi} d\chi \\ &= \int_0^{2\pi} \left(\frac{\delta E}{\bar{E}} - \frac{\delta u^r}{\bar{u}^r} \right) \frac{\bar{E}}{f} \frac{d\bar{\tau}}{d\chi} d\chi, \\ \delta\Phi &= \int_0^{2\pi} \left(\frac{\delta u^\phi}{\bar{u}^\phi} - \frac{\delta u^r}{\bar{u}^r} \right) \bar{u}^\phi \frac{d\bar{\tau}}{d\chi} d\chi \\ &= \int_0^{2\pi} \left(\frac{\delta L}{\bar{L}} - \frac{\delta u^r}{\bar{u}^r} \right) \frac{\bar{L}}{r^2} \frac{d\bar{\tau}}{d\chi} d\chi.\end{aligned}\quad (\text{A28})$$

Finally

$$\begin{aligned}\delta\Psi &= \int_0^{2\pi} \left(\frac{\delta\omega}{\bar{\omega}} - \frac{\delta u^r}{\bar{u}^r} \right) \bar{\omega} \frac{d\bar{\tau}}{d\chi} d\chi \\ &\equiv \int_0^{2\pi} [\delta_h + \delta_{\partial h} + c_{\delta E_{BS}}\delta E_{BS} + c_{\delta L_{BS}}\delta L_{BS}] \frac{d\bar{\tau}}{d\chi} d\chi,\end{aligned}\quad (\text{A29})$$

with

$$\begin{aligned}c_{\delta E_{BS}} &= -\frac{\bar{L}}{r^2} + \frac{(r^2 + \bar{L}^2)(3M-r)\bar{L}}{r^5(\bar{u}^r)^2}, \\ c_{\delta L_{BS}} &= \frac{\bar{E}}{r^2} - \frac{(3M-r)\bar{E}\bar{L}^2}{r^5(\bar{u}^r)^2}, \\ \delta_h &= \frac{\bar{E}\bar{L}}{2r^3} \left[(3M-r)h_{rr} - \frac{M}{f^2}h_{tt} - \frac{1}{r}h_{\phi\phi} \right] \\ &\quad + \left[\frac{(4M-r)\bar{L}}{rf}h_{tr} + \bar{E}h_{r\phi} \right] \frac{\bar{u}^r}{2r^2} \\ &\quad + \left[-\frac{(4M-r)\bar{E}^2}{f} + \frac{(5M-2r)\bar{L}^2}{r^2} \right. \\ &\quad \left. + (3M-r) \right] \frac{h_{t\phi}}{2r^3 f}, \\ \delta_{\partial h} &= \left[\left(\frac{h_{t[\phi,t]}}{f^2} + h_{r[\phi,r]} \right) \bar{E} \right. \\ &\quad \left. + \left(\frac{h_{\phi[\phi,t]}}{r^2 f} - h_{r[r,t]} \right) \bar{L} \right] \frac{\bar{u}^r}{r} \\ &\quad + \frac{\bar{E}^2 h_{t[\phi,r]} + (\bar{u}^r)^2 h_{r[\phi,t]}}{rf} + \frac{\bar{L}^2}{r^3} h_{\phi[t,r]} \\ &\quad - \left(\frac{h_{\phi[r,\phi]}}{r^2} + \frac{h_{t[r,t]}}{f} \right) \frac{\bar{E}\bar{L}}{r}.\end{aligned}\quad (\text{A30})$$

Appendix B: Self-force calculation

In order to obtain the metric perturbation we closely follow the approach of Kavanagh et al. [25], who used a radiation gauge and a related Teukolsky formalism. The set of PN solutions to the Teukolsky radial equation with $s = 2$ together with the Mano-Suzuki-Takasugi [43] solutions for $l = 2, \dots, 7$ are used to reconstruct the metric for $l \geq 2$. This allows one to compute the t and ϕ components of the conservative self-force needed to calculate the perturbed orbit quantities δE and δL , the induced shift of the orbital frequencies $\delta\Omega_r$ and $\delta\Omega_\phi$, the variation $\delta\Psi$ of the accumulated phase of the spin vector, and finally the spin-precession invariant $\Delta\psi$. The contribution of the multipoles $l = 0, 1$ corresponding to the spacetime perturbations due to the mass and angular momentum of the small body is computed separately. Finally, the so obtained value of $\delta\psi$ has to be regularized by subtracting out its singular part. We refer to Ref. [25] for a detailed account of all these intermediate steps and provide below only the relevant information about nonradiative multipoles, and the regularization parameter used in our analysis.

1. Low multipoles

The contribution of the lowest modes $l = 0, 1$ is obtained by using the solution for the interior and exterior perturbed metric given in Appendix A of Ref. [24] by

using the Regge-Wheeler-Zerilli approach. We find

$$\begin{aligned}\Delta\psi_{l=0}^+ &= \frac{(-1+2u_p)u_p^2(14u_p-3)}{(86u_p^2-39u_p+4)(-1+3u_p)} \\ &\quad - \frac{u_p^2(132888u_p^7-273260u_p^6+252318u_p^5-129169u_p^4+38665u_p^3-6710u_p^2+624u_p-24)}{2(-1+6u_p)(-1+3u_p)^2(86u_p^2-39u_p+4)^2(-1+2u_p)}e^2 + O(e^4), \\ \Delta\psi_{l=0}^- &= -\frac{(14u_p-3)u_p^3}{(86u_p^2-39u_p+4)(-1+3u_p)} \\ &\quad + \frac{(131460u_p^6-247960u_p^5+177821u_p^4-63837u_p^3+12278u_p^2-1210u_p+48)u_p^3}{2(-1+6u_p)(-1+3u_p)^2(86u_p^2-39u_p+4)^2(-1+2u_p)}e^2 + O(e^4),\end{aligned}\quad (B1)$$

and

$$\begin{aligned}\Delta\psi_{\ell=1}^+ &= -\frac{u_p(14u_p^3+55u_p^2-33u_p+4)}{(86u_p^2-39u_p+4)(-1+3u_p)} \\ &\quad + \frac{(261492u_p^7-583264u_p^6+518173u_p^5-241971u_p^4+65133u_p^3-10243u_p^2+880u_p-32)u_p^2}{(-1+6u_p)(-1+3u_p)^2(86u_p^2-39u_p+4)^2(-1+2u_p)}e^2 + O(e^4), \\ \Delta\psi_{\ell=1}^- &= \frac{2(-1+2u_p)(28u_p^2-17u_p+2)u_p}{(86u_p^2-39u_p+4)(-1+3u_p)} \\ &\quad - \frac{(531552u_p^7-980396u_p^6+772244u_p^5-337047u_p^4+87696u_p^3-13517u_p^2+1136u_p-40)u_p^2}{2(-1+6u_p)(-1+3u_p)^2(86u_p^2-39u_p+4)^2(-1+2u_p)}e^2 + O(e^4)\end{aligned}\quad (B2)$$

2. Regularization

To regularize the quantity $\Delta\psi$, it is enough to subtract the large- l limit of its PN expansion, i.e.,

$$\Delta\psi = \sum_{\ell=0}^{\infty} \left[\frac{1}{2} (\Delta\psi^{l,+} + \Delta\psi^{l,-}) - B \right], \quad (B3)$$

where the left and right contributions are such that $\Delta\psi^{l,+} = \Delta\psi^{-l-1,-}$ and

$$B(u_p, e) = B_0(u_p) + e^2 B_2(u_p), \quad (B4)$$

with

$$\begin{aligned}B_0(u_p) &= \frac{21}{16}u_p - \frac{201}{128}u_p^2 + \frac{529}{1024}u_p^3 + \frac{152197}{16384}u_p^4 + \frac{17145445}{262144}u_p^5 + \frac{88669225}{2097152}u_p^6 + \frac{45206277105}{16777216}u_p^7 \\ &\quad + \frac{9204713714385}{536870912}u_p^8 + \frac{1875482334818445}{17179869184}u_p^9 + O(u_p^{10}),\end{aligned}\quad (B5)$$

and

$$\begin{aligned}B_2(u_p) &= -\frac{435}{512}u_p^2 - \frac{1155}{1024}u_p^3 - \frac{352849}{65536}u_p^4 - \frac{5100243}{131072}u_p^5 - \frac{2456459237}{8388608}u_p^6 - \frac{36003649389}{16777216}u_p^7 \\ &\quad - \frac{32713771158557}{2147483648}u_p^8 - \frac{451723973383879}{4294967296}u_p^9 + O(u_p^{10}).\end{aligned}\quad (B6)$$

Acknowledgments

support and IHES for warm hospitality at various stages during the development of the present project.

DB thanks Chris Kavanagh for useful discussions. DB also thanks ICRA-Net and the Italian INFN for partial

[1] B. P. Abbott *et al.* [LIGO Scientific and Virgo Collaborations], “Observation of Gravitational Waves from a

Binary Black Hole Merger,” Phys. Rev. Lett. **116**, no.

6, 061102 (2016) doi:10.1103/PhysRevLett.116.061102 [arXiv:1602.03837 [gr-qc]].

[2] B. P. Abbott *et al.* [LIGO Scientific and Virgo Collaborations], “GW151226: Observation of Gravitational Waves from a 22-Solar-Mass Binary Black Hole Coalescence,” *Phys. Rev. Lett.* **116**, no. 24, 241103 (2016) doi:10.1103/PhysRevLett.116.241103 [arXiv:1606.04855 [gr-qc]].

[3] B. P. Abbott *et al.* [LIGO Scientific and Virgo Collaborations], “GW170814: A Three-Detector Observation of Gravitational Waves from a Binary Black Hole Coalescence,” *Phys. Rev. Lett.* **119**, no. 14, 141101 (2017) doi:10.1103/PhysRevLett.119.141101 [arXiv:1709.09660 [gr-qc]].

[4] B. P. Abbott *et al.* [LIGO Scientific and Virgo Collaborations], “GW170817: Observation of Gravitational Waves from a Binary Neutron Star Inspiral,” *Phys. Rev. Lett.* **119**, no. 16, 161101 (2017) doi:10.1103/PhysRevLett.119.161101 [arXiv:1710.05832 [gr-qc]].

[5] A. Buonanno and T. Damour, “Effective one-body approach to general relativistic two-body dynamics,” *Phys. Rev. D* **59**, 084006 (1999) doi:10.1103/PhysRevD.59.084006 [gr-qc/9811091].

[6] A. Buonanno and T. Damour, “Transition from inspiral to plunge in binary black hole coalescences,” *Phys. Rev. D* **62**, 064015 (2000) doi:10.1103/PhysRevD.62.064015 [gr-qc/0001013].

[7] T. Damour, P. Jaranowski and G. Schaefer, “On the determination of the last stable orbit for circular general relativistic binaries at the third postNewtonian approximation,” *Phys. Rev. D* **62**, 084011 (2000) doi:10.1103/PhysRevD.62.084011 [gr-qc/0005034].

[8] T. Damour, “Coalescence of two spinning black holes: an effective one-body approach,” *Phys. Rev. D* **64**, 124013 (2001) doi:10.1103/PhysRevD.64.124013 [gr-qc/0103018].

[9] T. Damour, B. R. Iyer, and A. Nagar, “Improved resummation of post-Newtonian multipolar waveforms from circularized compact binaries,” *Phys. Rev. D* **79**, 064004 (2009) doi:10.1103/PhysRevD.79.064004 [arXiv:0811.2069 [gr-qc]].

[10] A. Taracchini *et al.*, “Effective-one-body model for black-hole binaries with generic mass ratios and spins,” *Phys. Rev. D* **89**, no. 6, 061502 (2014) doi:10.1103/PhysRevD.89.061502 [arXiv:1311.2544 [gr-qc]].

[11] M. Pürller, “Frequency domain reduced order model of aligned-spin effective-one-body waveforms with generic mass-ratios and spins,” *Phys. Rev. D* **93**, no. 6, 064041 (2016) doi:10.1103/PhysRevD.93.064041 [arXiv:1512.02248 [gr-qc]].

[12] A. Bohé *et al.*, “Improved effective-one-body model of spinning, nonprecessing binary black holes for the era of gravitational-wave astrophysics with advanced detectors,” *Phys. Rev. D* **95**, no. 4, 044028 (2017) doi:10.1103/PhysRevD.95.044028 [arXiv:1611.03703 [gr-qc]].

[13] S. Khan, S. Husa, M. Hannam, F. Ohme, M. Pürller, X. Jiménez Forteza and A. Bohé, “Frequency-domain gravitational waves from nonprecessing black-hole binaries. II. A phenomenological model for the advanced detector era,” *Phys. Rev. D* **93**, no. 4, 044007 (2016) doi:10.1103/PhysRevD.93.044007 [arXiv:1508.07253 [gr-qc]].

[14] T. Damour and A. Nagar, “Effective One Body description of tidal effects in inspiralling compact binaries,” *Phys. Rev. D* **81**, 084016 (2010) doi:10.1103/PhysRevD.81.084016 [arXiv:0911.5041 [gr-qc]].

[15] S. Bernuzzi, A. Nagar, T. Dietrich and T. Damour, “Modeling the Dynamics of Tidally Interacting Binary Neutron Stars up to the Merger,” *Phys. Rev. Lett.* **114**, no. 16, 161103 (2015) doi:10.1103/PhysRevLett.114.161103 [arXiv:1412.4553 [gr-qc]].

[16] J. Steinhoff, T. Hinderer, A. Buonanno and A. Taracchini, “Dynamical Tides in General Relativity: Effective Action and Effective-One-Body Hamiltonian,” *Phys. Rev. D* **94**, no. 10, 104028 (2016) doi:10.1103/PhysRevD.94.104028 [arXiv:1608.01907 [gr-qc]].

[17] T. Damour, P. Jaranowski and G. Schäfer, “Nonlocal-in-time action for the fourth post-Newtonian conservative dynamics of two-body systems,” *Phys. Rev. D* **89**, no. 6, 064058 (2014) doi:10.1103/PhysRevD.89.064058 [arXiv:1401.4548 [gr-qc]].

[18] P. Jaranowski and G. Schäfer, “Derivation of local-in-time fourth post-Newtonian ADM Hamiltonian for spinless compact binaries,” *Phys. Rev. D* **92**, no. 12, 124043 (2015) doi:10.1103/PhysRevD.92.124043 [arXiv:1508.01016 [gr-qc]].

[19] T. Damour, P. Jaranowski and G. Schäfer, “Conservative dynamics of two-body systems at the fourth post-Newtonian approximation of general relativity,” *Phys. Rev. D* **93**, no. 8, 084014 (2016) doi:10.1103/PhysRevD.93.084014 [arXiv:1601.01283 [gr-qc]].

[20] T. Marchand, L. Bernard, L. Blanchet and G. Faye, “Ambiguity-Free Completion of the Equations of Motion of Compact Binary Systems at the Fourth Post-Newtonian Order,” arXiv:1707.09289 [gr-qc].

[21] T. Damour, P. Jaranowski and G. Schäfer, “Fourth post-Newtonian effective one-body dynamics,” *Phys. Rev. D* **91**, no. 8, 084024 (2015) doi:10.1103/PhysRevD.91.084024 [arXiv:1502.07245 [gr-qc]].

[22] D. Bini and T. Damour, “High-order post-Newtonian contributions to the two-body gravitational interaction potential from analytical gravitational self-force calculations,” *Phys. Rev. D* **89**, no. 6, 064063 (2014) doi:10.1103/PhysRevD.89.064063 [arXiv:1312.2503 [gr-qc]].

[23] D. Bini and T. Damour, “Two-body gravitational spin-orbit interaction at linear order in the mass ratio,” *Phys. Rev. D* **90**, no. 2, 024039 (2014) doi:10.1103/PhysRevD.90.024039 [arXiv:1404.2747 [gr-qc]].

[24] S. Hopper, C. Kavanagh and A. C. Ottewill, “Analytic self-force calculations in the post-Newtonian regime: eccentric orbits on a Schwarzschild background,” *Phys. Rev. D* **93**, no. 4, 044010 (2016) doi:10.1103/PhysRevD.93.044010 [arXiv:1512.01556 [gr-qc]].

[25] C. Kavanagh, D. Bini, T. Damour, S. Hopper, A. C. Ottewill and B. Wardell, “Spin-orbit precession along eccentric orbits for extreme mass ratio black hole binaries and its effective-one-body transcription,” *Phys. Rev. D* **96**,

no. 6, 064012 (2017) doi:10.1103/PhysRevD.96.064012 [arXiv:1706.00459 [gr-qc]].

[26] S. Akcay, D. Dempsey and S. R. Dolan, “Spin-orbit precession for eccentric black hole binaries at first order in the mass ratio,” *Class. Quant. Grav.* **34**, no. 8, 084001 (2017) doi:10.1088/1361-6382/aa61d6 [arXiv:1608.04811 [gr-qc]].

[27] D. Bini and T. Damour, “Analytic determination of high-order post-Newtonian self-force contributions to gravitational spin precession,” *Phys. Rev. D* **91**, no. 6, 064064 (2015) doi:10.1103/PhysRevD.91.064064 [arXiv:1503.01272 [gr-qc]].

[28] A. G. Shah and A. Pound, “Linear-in-mass-ratio contribution to spin precession and tidal invariants in Schwarzschild spacetime at very high post-Newtonian order,” *Phys. Rev. D* **91**, no. 12, 124022 (2015) doi:10.1103/PhysRevD.91.124022 [arXiv:1503.02414 [gr-qc]].

[29] C. Kavanagh, A. C. Ottewill and B. Wardell, “Analytical high-order post-Newtonian expansions for extreme mass ratio binaries,” *Phys. Rev. D* **92**, no. 8, 084025 (2015) doi:10.1103/PhysRevD.92.084025 [arXiv:1503.02334 [gr-qc]].

[30] T. Damour, “Gravitational Self Force in a Schwarzschild Background and the Effective One Body Formalism,” *Phys. Rev. D* **81**, 024017 (2010) doi:10.1103/PhysRevD.81.024017 [arXiv:0910.5533 [gr-qc]].

[31] D. Bini, T. Damour and A. Geralico, “New gravitational self-force analytical results for eccentric orbits around a Schwarzschild black hole,” *Phys. Rev. D* **93**, no. 10, 104017 (2016) doi:10.1103/PhysRevD.93.104017 [arXiv:1601.02988 [gr-qc]].

[32] E. Barausse, E. Racine and A. Buonanno, “Hamiltonian of a spinning test-particle in curved spacetime,” *Phys. Rev. D* **80**, 104025 (2009) Erratum: [Phys. Rev. D **85**, 069904 (2012)] doi:10.1103/PhysRevD.85.069904, 10.1103/PhysRevD.80.104025 [arXiv:0907.4745 [gr-qc]].

[33] D. Bini, T. Damour and A. Geralico, “Spin-dependent two-body interactions from gravitational self-force computations,” *Phys. Rev. D* **92**, no. 12, 124058 (2015) Erratum: [Phys. Rev. D **93**, no. 10, 109902 (2016)] doi:10.1103/PhysRevD.93.109902, 10.1103/PhysRevD.92.124058 [arXiv:1510.06230 [gr-qc]].

[34] T. Damour, P. Jaranowski and G. Schaefer, “Effective one body approach to the dynamics of two spinning black holes with next-to-leading order spin-orbit coupling,” *Phys. Rev. D* **78**, 024009 (2008) doi:10.1103/PhysRevD.78.024009 [arXiv:0803.0915 [gr-qc]].

[35] T. Damour, B. R. Iyer and B. S. Sathyaprakash, “Improved filters for gravitational waves from inspiralling compact binaries,” *Phys. Rev. D* **57**, 885 (1998) doi:10.1103/PhysRevD.57.885 [gr-qc/9708034].

[36] D. Bini and T. Damour, “Gravitational self-force corrections to two-body tidal interactions and the effective one-body formalism,” *Phys. Rev. D* **90**, no. 12, 124037 (2014) doi:10.1103/PhysRevD.90.124037 [arXiv:1409.6933 [gr-qc]].

[37] S. Akcay, L. Barack, T. Damour and N. Sago, “Gravitational self-force and the effective-one-body formalism between the innermost stable circular orbit and the light ring,” *Phys. Rev. D* **86**, 104041 (2012) doi:10.1103/PhysRevD.86.104041 [arXiv:1209.0964 [gr-qc]].

[38] L. Barack and N. Sago, “Gravitational self-force on a particle in eccentric orbit around a Schwarzschild black hole,” *Phys. Rev. D* **81**, 084021 (2010) doi:10.1103/PhysRevD.81.084021 [arXiv:1002.2386 [gr-qc]].

[39] A. Le Tiec, “First Law of Mechanics for Compact Binaries on Eccentric Orbits,” *Phys. Rev. D* **92**, no. 8, 084021 (2015) doi:10.1103/PhysRevD.92.084021 [arXiv:1506.05648 [gr-qc]].

[40] L. Barack and N. Sago, “Beyond the geodesic approximation: conservative effects of the gravitational self-force in eccentric orbits around a Schwarzschild black hole,” *Phys. Rev. D* **83**, 084023 (2011) doi:10.1103/PhysRevD.83.084023 [arXiv:1101.3331 [gr-qc]].

[41] N. Warburton, L. Barack and N. Sago, “Isofrequency pairing of geodesic orbits in Kerr geometry,” *Phys. Rev. D* **87**, no. 8, 084012 (2013) doi:10.1103/PhysRevD.87.084012 [arXiv:1301.3918 [gr-qc]].

[42] J.-A. Marck, “Solution to the equations of parallel transport in Kerr geometry; tidal tensor,” *Proc. R. Soc. A* **385**, 431 (1983) doi:10.1098/rspa.1983.0021

[43] S. Mano, H. Suzuki and E. Takasugi, “Analytic solutions of the Teukolsky equation and their low frequency expansions,” *Prog. Theor. Phys.* **95**, 1079 (1996) doi:10.1143/PTP.95.1079 [gr-qc/9603020].